Earth-Science Reviews 138 (2014) 156–178

Contents lists available at ScienceDirect

Earth-Science Reviews

journal homepage: www.elsevier.com/locate/earscirev

A comparison of detrital U–Pb zircon, $^{40}Ar/^{39}Ar$ hornblende, $^{40}Ar/^{39}Ar$ biotite ages in marine sediments off East Antarctica: Implications for the geology of subglacial terrains and provenance studies

E.L. Pierce [a,*], S.R. Hemming [a,b], T. Williams [b], T. van de Flierdt [c], S.N. Thomson [d], P.W. Reiners [d], G.E. Gehrels [d], S.A. Brachfeld [e], S.L. Goldstein [a,b]

[a] Department of Earth and Environmental Sciences, Columbia University, 116th Street & Broadway, New York, NY 10027, USA
[b] Lamont–Doherty Earth Observatory of Columbia University, Route 9W, Palisades, NY 10964, USA
[c] Department of Earth Science and Engineering, Imperial College London, South Kensington Campus, London SW7 2AZ, UK
[d] Department of Geosciences, University of Arizona, Tucson, AZ 85721, USA
[e] Department of Earth Environmental Studies, Montclair State University, 1 Normal Ave, Montclair, NJ 07043, USA

ARTICLE INFO

Article history:
Received 23 December 2013
Accepted 20 August 2014
Available online 28 August 2014

Keywords:
Thermochronology
Geochronology
Ice-rafted debris
Glacial diamict
Detrital zircon

ABSTRACT

U–Pb ages of detrital zircon grains have provided an extraordinary tool for sedimentary provenance work, given that they are ubiquitous, resistant to damage and weathering, and that the U–Pb age records the crystallization age of the mineral. Although not as widely used, $^{40}Ar/^{39}Ar$ dating of detrital hornblende and biotite grains can also serve as powerful sedimentary provenance tools, particularly in situations where chemical weathering is minor (e.g., Antarctica). Certain natural biases exist among these mineral chronometers (e.g., abundance in different rock types, durability during abrasion, resistance to dissolution) that determine the extent to which they are found in sedimentary deposits. Additionally, the $^{40}Ar/^{39}Ar$ systems in hornblende and biotite have lower closure temperatures for thermally activated diffusion (~500 °C and ~300 °C, respectively). Thus, for areas that have experienced a polymetamorphic history, such as East Antarctica, combining these approaches can provide added detail to provenance studies.

In this study we provide a comparison of the detrital U–Pb zircon, $^{40}Ar/^{39}Ar$ hornblende and $^{40}Ar/^{39}Ar$ biotite age populations from 28 glacial-diamict and glacial-marine sediment core samples located around East Antarctica (55°W to 163°E). We present 3370 new detrital age measurements of U–Pb zircon, $^{40}Ar/^{39}Ar$ hornblende, and $^{40}Ar/^{39}Ar$ biotite, in conjunction with previously published data from some of the same core sites, as well as 78 U–Pb zircon ages measured on dispersed zircons from five ice-rafted debris (IRD) layers recovered at ODP Site 1165. Our data indicate that detrital U–Pb zircon, $^{40}Ar/^{39}Ar$ hornblende and $^{40}Ar/^{39}Ar$ biotite ages faithfully document the onshore geology of source areas within East Antarctica, as expressed in their respective age populations. In addition, a number of previously unknown age populations are recorded by the combined thermochronometers. Assuming an East Antarctic provenance, this approach helps to identify otherwise hidden geologic provinces. Previously unrecognized age populations include Archean $^{40}Ar/^{39}Ar$ hornblende and biotite ages in Dronning Maud Land; 1200–1300 Ma $^{40}Ar/^{39}Ar$ hornblende ages in the Weddell Sea; ~1560 Ma population of U–Pb zircons from the Wilkes Land margin; and Grenvillian (1000–1200 Ma) U–Pb zircon ages from the Adélie/George V Land margin.

Contents

* Corresponding author.
E-mail addresses: epierce@ldeo.columbia.edu (E.L. Pierce), sidney@ldeo.columbia.edu (S.R. Hemming), trevor@ldeo.columbia.edu (T. Williams), tina.vandeflierdt@imperial.ac.uk (T. van de Flierdt), thomson@email.arizona.edu (S.N. Thomson), reiners@email.arizona.edu (P.W. Reiners), ggehrels@email.arizona.edu (G.E. Gehrels), brachfelds@mail.montclair.edu (S.A. Brachfeld), steveg@ldeo.columbia.edu (S.L. Goldstein).

http://dx.doi.org/10.1016/j.earscirev.2014.08.010
0012-8252/

1. Introduction

The U–Pb system in detrital zircons is a widely used and powerful tool for conducting sedimentary provenance studies (e.g., Gaudette et al., 1981; Andersen, 2005; Gehrels et al., 2011a; Gehrels, 2012, see Fedo et al. (2003) for a discussion of detrital U–Pb zircon studies). $^{40}Ar/^{39}Ar$ ages measured in detrital hornblende and biotite are less exploited as a sedimentary provenance tool, but they are increasingly being used for studies of ice rafted debris (IRD) around Antarctica and other regions characterized by tidewater glaciers (e.g., Gwiazda et al., 1996; Hemming et al., 1998; Hemming et al., 2000; Hemming and Hajdas, 2003; Peck et al., 2007; Roy et al., 2007b; Williams et al., 2010; Pierce et al., 2011; Downing et al., 2013; Knutz et al., 2013). In this study, we compare U–Pb zircon, $^{40}Ar/^{39}Ar$ hornblende and $^{40}Ar/^{39}Ar$ biotite ages measured on detrital mineral grains from glacially-derived marine sediment samples taken from 28 marine sediment cores located around East Antarctica (Figs. 1, 2).

The first objective is to provide a direct comparison of detrital zircon U–Pb, hornblende $^{40}Ar/^{39}Ar$ and biotite $^{40}Ar/^{39}Ar$ age populations. Given the natural biases that exist for each system (see Section 2), we are interested in which of the minerals are present, which age populations are present, if the age populations are present across all mineral systems, and how these ages relate to one another from a thermochronology point of view. The findings have broad implications for evaluating each of these chronometers as a provenance tracer around East Antarctica, and they will particularly benefit the study IRD. The provenance of IRD provides key information on the ice sheet and ocean circulation dynamics that transport the mineral grains from their source to the ocean floor: flowing ice erodes and incorporates debris, and when the ice streams reach the ocean, they calve off icebergs that are carried by ocean currents, melting as they travel, and causing the entrained debris to sink and be deposited on the ocean floor.

The second objective of this study is to use this information to increase our understanding of East Antarctica's geology. Today more than 98% of East Antarctica is covered by the thick East Antarctic ice sheet, and relatively little outcrop is available for direct geologic study (Fig. 2). Despite these challenges, the general geological history of East Antarctica is known reasonably well. The bulk of East Antarctica was formed during the Precambrian; it comprises a number of Archean cratons, surrounded by orogenic belts and accreted terranes of Proterozoic and younger ages (e.g., Tingey, 1991; Boger, 2011). The amalgamation of the continents to form the supercontinent Rodinia at ~1100 Ma led to widespread occurrence of terranes with approximately Grenvillian (900–1300 Ma) ages. Though the Grenville orogeny itself is defined by Mesoproterozoic collisional activity along the Laurentian margin (e.g., Rivers, 1997), Fitzsimons (2000) compiled available U–Pb zircon outcrop data from East Antarctica and previous contiguous margins (see Fitzsimons (2000) for full description of data used), and defined three distinct Grenville-aged (or Grenvillian) zones in East Antarctica: Dronning Maud Land (1030–1090 Ma), Prydz Bay or Rayner Province (900–990 Ma), and Wilkes Land (1130–1330 Ma). In this paper we follow suit and refer to age populations within the bounds of 900 to 1330 Ma as Grenvillian or Grenville-aged. The timing of the subsequent break-up of Rodinia remains controversial (as does the existence of Rodinia itself), with different studies arguing for different ranges of ages that span ages from 520 to 1000 Ma, and for either continuous or multiphase rifting (Goodge et al., 2002; Cordani et al., 2003; Meert and Torsvik, 2003; Veevers, 2004).

A re-assembly of the continents occurred after rifting, with East Gondwana (India, Australia, and East Antarctica) colliding with West Gondwana (South America and Africa) to form Gondwanaland. During this time of continental amalgamation, two temporally close orogenies, the Pan-African and the Ross-Beardmore, affected the East Antarctic Craton (EAC).

The Pan-African orogeny (500–650 Ma) was the result of the Gondwana blocks colliding to form Gondwana, while the Ross orogeny (~480–590 Ma) was the result of subduction between Gondwana and what would become the Pacific plate (Tingey, 1991; Goodge, 2007; Boger, 2011). During these partly contemporaneous orogenies, the continued attachment of East Antarctica, India and Australia meant that parts of the craton – specifically Wilkes Land and part of Adélie Land – were buffered from the intense tectonothermal activity associated with these orogenies. The evidence for this buffering is the lack of a high-temperature overprint signatures in the ages of in-situ and detrital

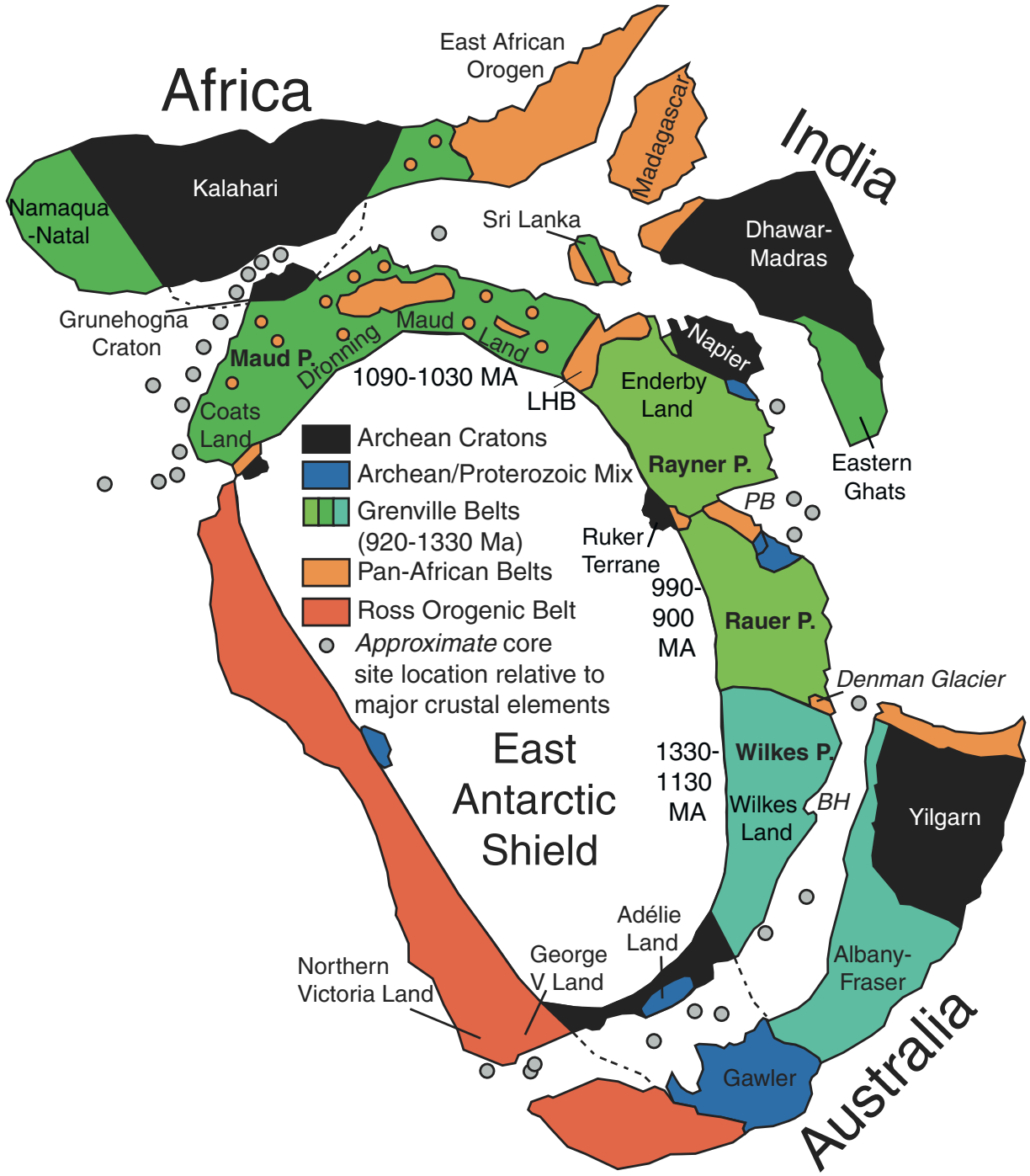

Fig. 1. East Antarctic crustal provinces and approximate core sites. Map modified from Harley and Kelly (2007); Grenvillian age ranges are as defined by Fitzsimons (2000). BH — Bunger Hills, DG — Denman Glacier, EG — Eastern Ghats, GC — Grunehogna Craton, GVL — George V Land, LHN — Lützow–Holm Belt, NVL — northern Victoria Land, P — Province, PB — Prydz Bay, R — Ruker Terrane, SL — Sri Lanka. (For the color version of this figure, the reader is referred to the web version of this article.)

zircons and hornblendes; these parts of East Antarctica still maintain Grenvillian and Paleoproterozoic ages based on $^{40}Ar/^{39}Ar$ hornblende and U–Pb zircon dates (Tingey, 1991; Anderson, 1999; Peucat et al., 1999; Fitzsimons, 2000; Di Vincenzo et al., 2007; Roy et al., 2007b; Pierce et al., 2011). This geologic history has left East Antarctica with dominant, characteristic high temperature age populations of ~3.0 Ga (cratons), 900–1300 Ma (Grenvillian) and 400–600 Ma (Pan-African/Ross orogenies) (Fig. 1). Examining the populations of U–Pb and $^{40}Ar/^{39}Ar$ ages in glacial-marine sediments deposited around East Antarctica will allow us to augment these broad interpretations with additional details on the thermochronology and hence geology of the unexplored parts of East Antarctica covered by the vast ice sheet.

2. Zircon, hornblende and biotite in provenance studies

There are some fundamental differences between the ages reflected by U–Pb measured in zircon and $^{40}Ar/^{39}Ar$ measurements in hornblende and biotite. Some of the basic advantages to using U–Pb zircon ages as a provenance tracer of terrestrial deposits, e.g., sandstones, do not hold true for provenance studies of marine sediments recovered in polar regions, and vice-versa. Here we provide a brief description of these

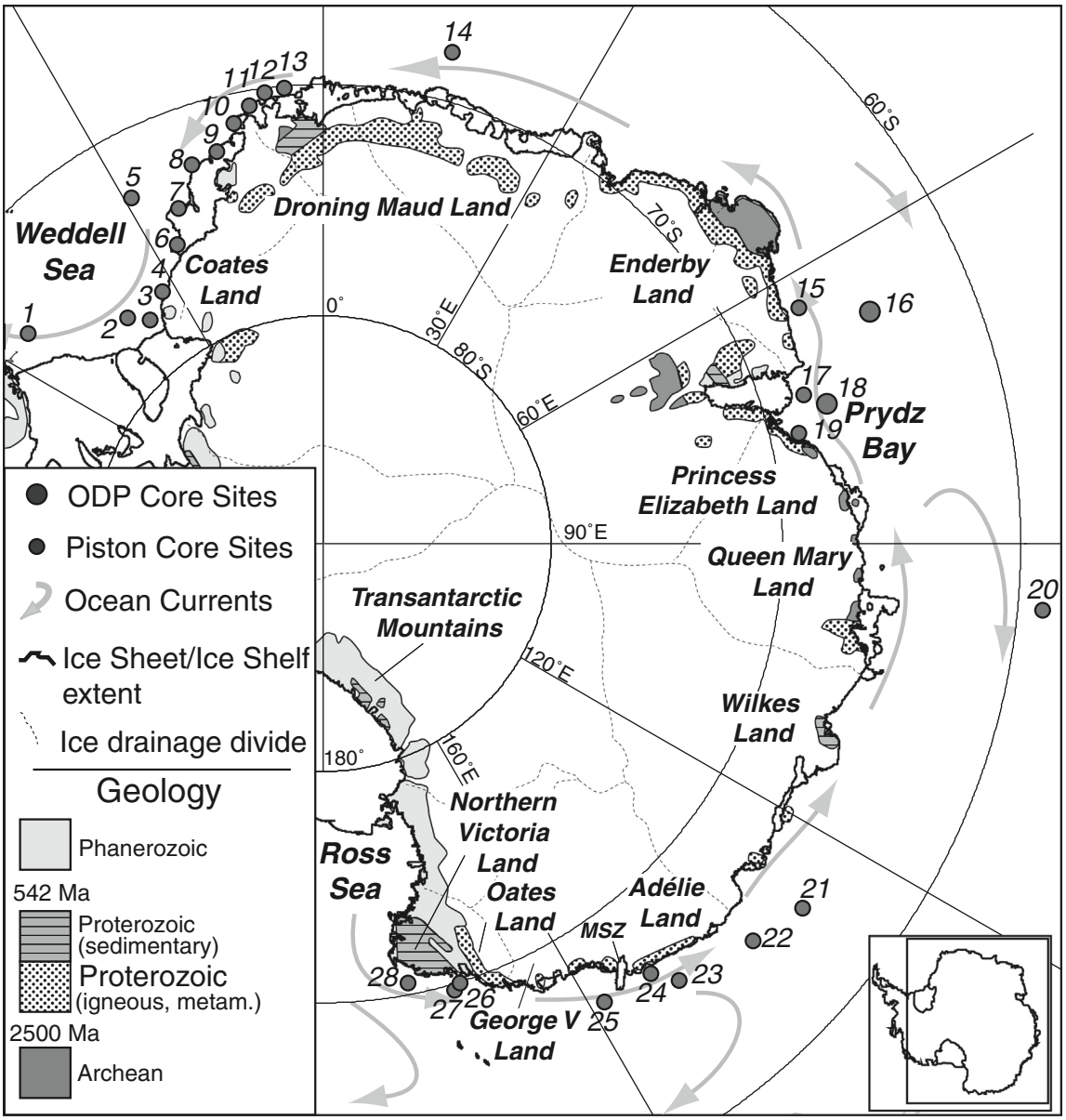

Fig. 2. Location map of East Antarctica showing outcrops, simplified geology, ocean currents and cores sites. Geology from Collins and Pisarevsky (2005).

generally known differences, in order to highlight why the U–Pb zircon, $^{40}Ar/^{39}Ar$ hornblende and $^{40}Ar/^{39}Ar$ biotite age populations found in a sediment sample may not always provide the same view of provenance.

2.1. Occurrence of zircon, hornblende and biotite in different rock types

Zircon, hornblende and biotite occur in varying amounts in different rock types, a fact that should be taken into account when considering provenance tools. Zircon ($ZrSiO_4$) is an accessory mineral found in trace amounts in most types of igneous and metamorphic rocks, is most common in felsic crystalline rocks (e.g., granitoids) and orthogneisses, and is highly concentrated in mature sandstones (Table 1). Hornblende (general formula $Ca_2Mg_4(Al,Fe^{3+})(Al,Si)_8O_{22}(OH)_2$), a member of the amphibole group, is a major-rock forming mineral found in high concentrations in intermediate igneous rocks, e.g., diorite, as well as medium- to high-grade metamorphic rocks (e.g., amphibolite facies), especially in mafic/ultramafic protoliths. Hornblende does not usually occur as a major mineral in the sedimentary rock record because it is weathered relatively easily, and is usually incorporated into the clasts in clastic sedimentary rocks, e.g., conglomerates. Biotite ($K(Mg,Fe)_3(AlSi_3O_{10})(OH_2)$), a mica, is a major rock-forming mineral found in high concentrations in felsic-intermediate igneous rocks, e.g., granitoids and diorite, and low- to medium-grade metamorphic rocks, e.g., hornfels, phyllite and schist. Biotite also is not a major detrital mineral in the sedimentary rock record, though it tends to be more abundant than hornblende (Deer et al., 1992).

2.2. Weathering

In terms of relative susceptibility to chemical and physical weathering, zircon is most resistant, then biotite, then hornblende (Goldich, 1938; Kowalewski and Rimstidt, 2003). Zircon is one of the most refractory minerals, and is common in both modern and ancient sedimentary environments. It is highly resistant to both chemical and physical weathering during erosional processes and subsequent burial, primarily due to its crystal structure with tightly bonded SiO_4 tetrahedra (Thoulet, 1913; Boswell, 1923; Goldich, 1938; Pettijohn, 1941; Morton, 1984; Bateman and Catt, 1985; Morton, 1991). Zircon not only survives

Table 1
Relative concentrations of zircon, hornblende and biotite in major lithologies (Poldervaart, 1955, 1956; Deer et al., 1992; Nesse, 2000; Reiners et al., 2005b).

Zircon	High	Medium	Low to none
Igneous	Felsic crystalline (granite, granodiorite, tonalite)	Rhyolite, ignimbrite	Gabbro, basalt, ultramafic
Metamorphic	Orthogneiss	Paragneiss, metarhyolite, metasandstone, phyllite	Marble, eclogite, schist
Sedimentary	Arkose	Conglomerate, quartz-arenite, litharenite	Claystone, dolomite, carbonate rocks
Hornblende	High	Medium	Low to none
Igneous	Intermediate rocks; granodiorite, diorite	Granite, gabbro	Ultramafic
Metamorphic	Medium to high-grade; mafic/ultramafic protolith	Medium grade	Marble, carbonate protolith
Sedimentary	None	None	Clastics
Biotite	High	Medium	Low to none
Igneous	Felsic rocks; granite, rhyolite	Intermediate and mafic rocks, diorite, andesite	Ultramafic
Metamorphic	Low to intermediate grade; hornfels, phyllites, schists and gneisses	High grade; migmatites	Mafic protolith
Sedimentary	None	None	Clastics, immature sediments

sedimentary transport well, but also can survive through multiple cycles of burial, orogenesis, and erosion. Indeed, Kowalewski and Rimstidt (2003) have zircon ranked as the most durable detrital mineral. A zircon population in the sedimentary environment can record several tectonic events, which makes the interpretation of detrital zircon populations for provenance studies often challenging. For example, samples may contain recycled zircons that were transported from an original location of formation to a secondary location, and then eroded more recently from the secondary location, but with a provenance signal indicating the original location. As has been discussed before, (e.g., Thomas, 2011), the fact that zircon survives through many sedimentary cycles is an advantage, because a zircon population can record several tectonic events. However, it is also a challenge when interpreting detrital zircon populations for provenance studies, because samples may contain recycled zircons.

While both biotite and hornblende may also be found in modern and ancient sedimentary deposits, their susceptibility to weathering makes the occurrence of un-weathered/un-altered grains unusual, particularly in modern environments with high chemical weathering rates, or in ancient sediments. Both hornblende and biotite are ferromagnesian silicates, and as such are susceptible to chemical weathering via oxidation. Hornblende is, however, slightly more susceptible to weathering than biotite, as discussed by Goldich (1938), and as explained by their relative placement on Bowen's reaction series (Bowen, 1922). Hornblende forms at a higher temperature than biotite, its bonds are not as strong as those of biotite, and thus it breaks down more readily. Biotite can generally survive transport for long distances in modern sedimentary systems, as its elastic nature protects it from abrasion (Kowalewski and Rimstidt, 2003; Hodges et al., 2005). However, biotite is very susceptible to chemical dissolution. Hornblende and biotite typically survive through only one sedimentary cycle and thus the application of $^{40}Ar/^{39}Ar$ ages in these minerals to provenance studies is more straightforward.

2.3. Geochronology and thermochronology

Typically, zircon core ages represent the age of crystallization, and are rarely if ever reset during successive tectonothermal events (e.g., Mezger and Krogstad, 1997), but rims can often grow around the original crystal during successive orogenies or later magma crystallization (Silver and Deutsch, 1963; Bickford et al., 1981). Lead loss, by various means (see Mezger and Krogstad, 1997), can lead to discordant U–Pb ages. Conversely, zircons with high U concentrations can turn metamict, which can result in preferential destruction of this type of zircon.

In contrast to the retention of their initial crystallization ages that characterizes zircon, $^{40}Ar/^{39}Ar$ ages measured in hornblende reflect the time since the hornblende grain most recently formed or cooled below ~500 °C (McDougall and Harrison, 1999). As a result, the $^{40}Ar/^{39}Ar$ age of hornblende records the last major tectonothermal event experienced by its host rock. Similarly, the $^{40}Ar/^{39}Ar$ ages measured in biotite reflect the time since the biotite grain formed or cooled below ~300 °C, and thus it is more likely than hornblende to record minor tectonothermal events (Reiners et al., 2005b).

2.4. Transport mechanisms

The transport mechanisms and depositional environments of sediments need to be considered when conducting sedimentary provenance studies. Below is a summary of studies that apply the detrital U–Pb zircon, $^{40}Ar/^{39}Ar$ hornblende and $^{40}Ar/^{39}Ar$ biotite ages to provenance studies in glacial and non-glacial environments. See Tables 2A and 2B for a list of non-glacial terrestrial provenance studies (A) and glacial-marine and terrestrial provenance studies (B) that apply these methods, and which summarize the studies mentioned in Sections 2.4.1 and 2.4.2.

2.4.1. Terrestrial sediment provenance studies in non-glacial environments

Previous detrital U–Pb zircon provenance studies are too numerous to mention here as a comprehensive list, attesting to the strength of this tool from its earliest uses (e.g., Ledent et al., 1964; Tatsumoto and Patterson, 1964; Gaudette et al., 1981) to more recent studies (e.g., Gehrels et al., 2011a; Gehrels, 2012; see Fedo et al. (2003) for a discussion of detrital U–Pb zircon studies). Typically, these studies are based on sediments that were eroded, transported and deposited by wind or water; transport mechanisms that ultimately sort sediments, which, paired with the resilient nature of zircon, serve to concentrate zircons.

As discussed above, biotite and hornblende are not as resilient as zircon, and so the $^{40}Ar/^{39}Ar$ ages of biotite and hornblende have not been exploited as a provenance tool as much as detrital zircon U–Pb (Table 2A). Where they have been applied to terrestrial studies, the results on $^{40}Ar/^{39}Ar$ ages of detrital biotite have been variably successful. Renne et al. (1990) applied detrital $^{40}Ar/^{39}Ar$ biotite ages to constrain the provenance of the Eocene Montgomery Creek Formation in northern California, however biotite grains were found to contain vermiculite as interlayer laminations and rinds, which lowered the integrated age of the biotite grains; accordingly, the $^{40}Ar/^{39}Ar$ biotite ages were not used as a tracer of provenance in this study. Cohen et al. (1995) successfully applied the $^{40}Ar/^{39}Ar$ ages of detrital hornblende and step-heated biotite grains in volcaniclastic Jurassic sandstones in southern Alaska, in order to determine the provenance of the Seymour Canal Formation. In this case, weathering was a minor factor and grains were selected based upon their physical appearance of little to no alteration. The authors were able to conclude that the biotite grains were sourced from the volcanic arc of the Gravina Belt. Aalto et al. (1998) applied the $^{40}Ar/^{39}Ar$ ages of detrital biotite to determine the provenance of Eocene–Miocene Hoh assemblage sandstones in northern California. These authors found that the detrital $^{40}Ar/^{39}Ar$ biotite ages they measured did not yield meaningful ages, as the ages were widely scattered,

Table 2A
Provenance studies of terrestrial non-glacial sediments using U–Pb zircon, $^{40}Ar/^{39}Ar$ hornblende and $^{40}Ar/^{39}Ar$ biotite ages.

$^{40}Ar/^{39}Ar$ biotite					
Study	Material	Location	Purpose of study	Results	Why?
Aalto et al., 1998	Eocene–Miocene Hoh assemblage sandstones	Hoh assemblage, northern California	Determining the provenance of Eocene–Miocene Hoh assemblage sandstones	Unsuccesful	Biotites: ages widely scattered, incrementally heated grains did not form plateaus, radiogenic Ar < 20%.
Cohen et al., 1995	Late Jurassic–mid Cretaceous Volcaniclastic sandstones	Gravina Belt, southeastern Alaska	Determining provenance of the Seymour Canal Formation	Successful	Samples were chosen based upon degree of weathering (picked those with least degree of weathering); grains were hand-picked with a binocular microscope and any visibly altered grains were rejected. Both approaches gave meaningful results; weathering and alteration of grains was minor.
Renne et al., 1990	Montgomery creek sandstones	Montgomery creek formation, northern California	Provenance of the Eocene montgomery creek formation	Unsuccessful	Biotite ages were widely scattered; determined to contain increasing amounts of vermiculite as interlayer lamintations and as rinds on the grain which increased with depth; this lowers the integrated Ar/Ar age of the biotite grains.
$^{40}Ar/^{39}Ar$ Hornblende					
Study	Material	Location		Results	Why?
Cohen et al., 1995	Late Jurassic–mid Cretaceous volcaniclastic sandstones	Gravina Belt, southeastern Alaska	Determining provenance of the Seymour Canal Formation	Successful	Samples were chosen based upon degree of weathering (picked those with least degree of weathering); grains were hand-picked with a binocular microscope and any visibly altered grains were rejected. Both approaches gave meaningful results; weathering and alteration of grains was minor.
U–Pb Zircon					
See reviews in Gehrels (2012), Gehrels et al. (2011b); Fedo et al. (2003).					

no plateau ages were reached during incremental step-heating of the grains, and radiogenic argon was <20% in most samples, all indicating chemical alteration of the grains. Thus, in terrestrial provenance, weathering of the mineral grains can degrade or destroy the $^{40}Ar/^{39}Ar$ signal, but reliable ages and provenance can be determined on grains where weathering/alteration/dissolution is minor.

2.4.2. Terrestrial and marine sediment provenance studies in glacial environments

Some of the basic advantages of detrital zircon U–Pb ages and disadvantages of hornblende and biotite $^{40}Ar/^{39}Ar$ ages as provenance tracers of terrestrial deposits do not apply to provenance studies of terrestrial and marine sediments recovered from the polar regions. In polar regions, and especially in East Antarctica, the dominant style of weathering is mechanical, and the majority of sedimentary provenance studies aim to determine the sources of IRD. Unlike wind and water, glacial transport does not sort sediment. In glacial–fluvial settings, however, material comminuted by ice and subsequently entrained in water may undergo some hydraulic sorting. This process will mostly affect biotite grains, and concentrate them in the finer sediment fractions (Nesbitt and Young, 1996). In ice-dominated transport systems, the lack of fluvial hydraulic sorting paired with the low amount of chemical weathering means that there should be no significant preferential concentration of zircon relative to hornblende relative to biotite, such that these minerals should more closely approximate the proportions in the source lithologies that were eroded.

In IRD and other glaciogenic sediment used for provenance studies, the $^{40}Ar/^{39}Ar$ age of detrital biotite is emerging as promising provenance tool. As a potassium-bearing mineral, biotite in the 63–150 μm fraction, in addition to the >150 μm fraction, contains measurable amounts of argon, increasing the number of potential grains in a given sample that can be used for thermochronology. In the North Atlantic, Hemming et al. (2002) measured the $^{40}Ar/^{39}Ar$ ages of a small number of ice-rafted biotite grains, which indicated a provenance of the IRD similar to the mid-Norwegian provenance indicated by the ice-rafted $^{40}Ar/^{39}Ar$ hornblende ages presented in the same study. van de Flierdt et al. (2008) applied the $^{40}Ar/^{39}Ar$ ages of detrital biotite from fluvial and glacial-marine sediments recovered at ODP Site 1166 in Prydz Bay, East Antarctica, to investigate the origin of the Gamburtsev Subglacial Mountains, and showed that these mountains could not be of a young volcanic origin. Pierce et al. (2011) found that the $^{40}Ar/^{39}Ar$ ages of ice-rafted biotite grains can be applied as a tracer of IRD provenance around the Wilkes and Adélie Land margins of East Antarctica; $^{40}Ar/^{39}Ar$ biotite ages used to characterize source areas reflected what is known through outcrop studies, and a comparison of ice-rafted $^{40}Ar/^{39}Ar$ biotite and $^{40}Ar/^{39}Ar$ hornblende ages (Williams et al., 2010) at ODP Site 1165 demonstrated that the $^{40}Ar/^{39}Ar$ biotite ages indicated the same provenance sectors as the previously published $^{40}Ar/^{39}Ar$ biotite hornblende ages (Williams et al., 2010). Around East Antarctica, Pierce et al. (2011) found that there were a large numbers of grains that showed no signs of chemical alteration and gave robust ages. Palmer et al. (2012) successfully applied $^{40}Ar/^{39}Ar$ dating of biotite to glacial tills and cobbles in the Transantarctic Mountains in order to study the subglacial geology of this area.

In IRD and other glaciogenic sediment provenance studies, the $^{40}Ar/^{39}Ar$ of detrital hornblende has also been demonstrated as a reliable provenance tool (Table 2A). Studies in the North Atlantic (Gwiazda et al., 1996; Hemming et al., 1998; Hemming et al., 2000; Hemming et al., 2002; Hemming and Hajdas, 2003; Peck et al., 2007; Downing et al., 2013; Knutz et al., 2013) and in the circum-Antarctic (Roy et al., 2007b; van de Flierdt et al., 2008; Williams et al., 2010; Pierce et al., 2011; Tochilin et al., 2012) have successfully applied the

Table 2B
Provenance Studies of glacial sediments (till, ice-rafted detritus) using U–Pb zircon, $^{40}Ar/^{39}Ar$ hornblende and $^{40}Ar/^{39}Ar$ biotite ages.

$^{40}Ar/^{39}Ar$ biotite

Study	Sample type	Location	Purpose of study
Hemming et al., 2002	Glacial marine/trough mouth fans	North Atlantic	Tracing IRD provenance during Heinrich Events
van de Flierdt et al., 2008	Glacial marine and fluvial sediments	East Antarctica, Prydz Bay, ODP Site 1166A	Investigating the origin of the subglacial Gamburtsev Mountains
Pierce et al., 2011	Glacial-marine sediments; ice-rafted detritus and diamict	East Antarctica; ODP Site 1165	Characterizing geology and IRD source areas around in East Antarctica.
Palmer et al., 2012	Glacial till	Transantarctic Mountains	Characterizing subglacial geology.

$^{40}Ar/^{39}Ar$ hornblende

Study	Sample type	Location	Purpose of study
Gwiazda et al., 1996	Glacial-marine sediments; ice-rafted detritus	North Atlantic	Tracing IRD provenance during Heinrich Events
Hemming et al., 1998	Glacial-marine sediments; ice-rafted detritus	N.E. Atlantic (V28-82)	Tracing IRD provenance during Heinrich Events
Hemming et al., 2000	Glacial-marine sediments; ice-rafted detritus	North Atlantic (EW9303-GGC31)	Tracing IRD provenance 22 to 10.5 ka BP
Hemming et al., 2002	Glacial marine/trough mouth fans	North Atlantic	Tracing IRD provenance during Heinrich Events
Hemming and Hajdas, 2003	Glacial-marine sediments; ice-rafted detritus	North Atlantic (V23-14)	Tracing IRD provenance over the past 43 ^{14}C kyr
Roy et al., 2007b	Glacial-marine sediments; ice-rafted detritus	Antarctica; multiple sites	Characterizing geology around Antarctica
Roy et al., 2007a	Glacial till	North Central USA	Tracing provenance of tills over the past ~2.0 Ma
Peck et al., 2007	Glacial-marine sediments; ice-rafted detritus	North Atlantic (MD01-2461)	Tracing IRD provenance during Heinrich Events
van de Flierdt et al., 2008	Glacial marine and fluvial sediments	East Antarctica, Prydz Bay, ODP Site 1166A	Investigating the origin of the subglacial Gamburtsev Mountains
Williams et al., 2010	Glacial-marine sediments; ice-rafted detritus	East Antarctica ODP Site 1165	Tracing IRD provenance during Heinrich-like events
Pierce et al., 2011	Glacial-marine sediments; ice-rafted detritus and diamict	East Antarctica; multiple sites	Characterizing IRD source areas around in East Antarctica
Palmer et al., 2012	Glacial till	Transantarctic Mountains	Characterizing subglacial geology
Tochilin et al., 2012	Glacial marine sediments; diamictite	East Antartica, ODP Site 739	Determining Early Oligocene through Quaternary erosion rates in East Antarctica
Downing et al., 2013	Glacial-marine sediments; ice-rafted detritus	North Atlantic	Tracing IRD provenance during Heinrich Events
Knutz et al., 2013	Glacial-marine sediments; ice-rafted detritus	North Atlantic/Greenland	Tracing IRD provenance during the last glacial–interglacial transition

U–Pb Zircon

Study	Sample type	Location	Purpose of study?
Avigad et al., 2007	Glacial diamictite	Ethiopia, Negash Syncline	Determining provenance and chronolgy of Cyrogenian diamictites
van de Flierdt et al., 2008	Glacial marine and fluvial sediments	East Antarctica, Prydz Bay, ODP Site 1166A	Investigating the origin of the subglacial Gamburtsev Mountains
Goodge and Fanning, 2010	Glacial-marine sediments	East Antarctica, Adélie Land Margin	Characterizing subglacial geology
Goodge et al., 2010	Glacial till	Transantarctic Mountains	Characterizing subglacial geology
Gehrels et al., 2011a	Glacial diamicite	Tibetan Himalyans	Constraining paleogeogprahy and tecontic history of Mesoproterozoic through Mesozoic Tibet–Himalaya region
Veevers and Saeed, 2011	Glacial-marine sediments; turbidites	East Antarctica, DSDP Sites 268, 269, 273 and 274	Comparison of onland and detrital U–Pb zircon ages to improve udnerstanding of East Antarctic geology
Palmer et al., 2012	Glacial till	Transantarctic Mountains	Characterizing subglacial geology
Tochilin et al., 2012	Glacial diamictite	East Antartica, ODP Site 739	Determining Early Oligocene through Quaternary erosion rates in East Antarctica
Small et al., 2013	Glacial-marine sediments; ice rafted detritus	North Atlantic, Site MD95-2007	Determining IRD provenance during the Younger and Older Dryas events and testing viaibliy of U–Pb zircon and U–Pb rutile as IRD tracers

$^{40}Ar/^{39}Ar$ tool. In glacial till samples, this method has been successfully applied both in Antarctica and North America. Roy et al. (2007a) used detrital $^{40}Ar/^{39}Ar$ hornblende ages from mid-continent till samples to constrain Laurentide ice sheet extent during the past ~2.0 Ma. They showed that a consistent source of till deposited during ice sheet advances over the past ~2 Myr was the northwestern Keewatin sector of the Laurentide ice sheet, indicating the sustained presence of an ice dome in that area. Palmer et al. (2012) successfully applied $^{40}Ar/^{39}Ar$ dating to hornblende in glacial till deposits from the Transantarctic Mountains with the goal of studying subglacial geology, Tochilin et al. (2012) presented detrital hornblende $^{40}Ar/^{39}Ar$ ages from Oligocene to recent glacial sediments in the Prydz Bay sector of East Antarctica to look at long term tectonic and erosion history in the Lambert Graben region of East Antarctica. Combined with other thermochronometers (see Section 7), they were able to infer that erosion rates slowed from a relatively high rate in the Oligocene (following East Antarctic ice-sheet initiation), to relatively low rates from the late Miocene onwards.

In glaciogenic sediment provenance studies using the U–Pb zircon method, most work has been restricted to terrestrial samples, though increasingly studies are using glacial-marine samples (Table 2A). van de Flierdt et al. (2008), Tochilin et al. (2012), and Palmer et al. (2012), in the studies discussed above, also measured detrital U–Pb zircon ages. Goodge et al.(2010) measured U–Pb ages on zircons from Neogene and Quaternary till clasts deposited in the central Transantarctic Mountains, and, based on Grenvillian U–Pb zircon ages, provided evidence for the extension of Grenville-aged crust into East Antarctica along the Ross-Sea margin. Goodge and Fanning (2010) measured U–Pb ages on detrital zircons from glacial-marine sediments (dispersed and from clasts) from western Wilkes Land; while age populations were dominated by a Ross signature, many older age populations show both the importance of this approach to identifying the age of un-exposed basement rocks, as well as the presence of older (Neoproterzoic, Mesoproterozoic and Archean) terranes within the interior of East Antarctica adjacent to western Wilkes Land. In a review of U–Pb zircon ages and various geochemical proxies from around East Antarctica, Veevers and Saeed (2011) measured detrital U–Pb zircon ages from sediments offshore of East Antarctica (glacial diamict and turbidites, respectively), which offered valuable insights to the obscured subglacial

geology of East Antarctica's interior. These authors argue that the East Antarctic craton is dominated by igneous and metamorphic ages of ~500–700, 900–1300, 1400–1700, 1900–2100, 2200–2300, 2600–2800, and 3150–3350 Ma.

Recent work in the North Atlantic (Small et al., 2013) applied U–Pb measurements on ice-rafted zircons to determine the provenance of IRD during the last deglacial period. Though the number of zircons was small, the authors inferred provenance with the additional pairing of U–Pb ages on ice-rafted rutile, and concluded that the IRD was sourced from the Laurentia, as opposed to Scotland, which is closer to the core site, indicating rapid distribution of IRD during the Older Dryas Cold Reversal. To our knowledge no studies have attempted to use U–Pb ages of ice-rafted zircons to determine the provenance of IRD in the Southern Ocean. Detrital U–Pb zircon provenance studies have also been applied to pre-Cenozoic glacial deposits. For example, Avigad et al. (2007) determined the provenance of Cryogenian diamictites from northern Ethiopia using this method while Gehrels et al. (2011b) determined Carboniferous–Permian diamictite provenance from the Tibet–Himalayan orogeny.

Another important consideration for determining the provenance of IRD is sample size. Detrital zircon studies are most often applied to determining the provenance of sandstones and conglomerates, and the general practice is to take large samples in order to obtain sufficient zircons; Gehrels et al. (2006) advocate taking 4.5 to 18 kg samples for detrital U–Pb zircon provenance studies, depending on the maturity of the sandstone. It is important to note that for a terrestrial setting, sample size is generally not restricted by the availability of the material. Sample sizes taken from marine sediment cores for the purpose of studying IRD, however, are typically 10–20 cm^3, a size dictated by sedimentation rates in the open ocean (and thus the depositional age range of the interval sampled) and the fact that the diameter of a sediment core is typically ~6 cm. Furthermore, the bulk of pelagic marine sediments is typically in the <63 μm fraction, in which case major rock forming minerals are more likely to provide abundant grains for analysis.

3. Approach and sampling sites

There are essentially two provenance components to this study. The first is making the connection between the samples taken from the core sites to known outcrops on-land; the provenance of these samples should be more localized to the ice-sheet drainage that delivers material to the core site, as subglacial till or by local ice-rafting (Fig. 2). The second is to investigate changes through time in the provenance of ice-rafted grains from an open-ocean core site, located ~400 km away from the coast (ODP Site 1165, see Fig. 2). The provenance of the ice-rafted material delivered to such a site has the potential to reflect sourcing from both local and distant sources, depending on past climatic conditions (e.g., sea-surface temperatures controlling the rate of melting of the icebergs, ocean currents, wind, and ice-sheet behavior).

For this study, we compare U–Pb zircon, $^{40}Ar/^{39}Ar$ hornblende, and $^{40}Ar/^{39}Ar$ biotite ages from 28 marine sediment core sites (Figs. 1, 2). Table 3 contains a full description of core site locations, water depth, sample type, and sampling depth. Samples from twenty-seven of the core sites were analyzed using each of the mineral systems, with the goal of studying subglacial geology and refining the characterization of potential IRD sources. Multiple layers were analyzed in several cores in order to increase the number of analyses for each mineral system. Samples from 26 of the core sites were provided by Florida State University's Antarctic Marine Geology Research Facility (FSU AMGRF), and consist of piston or jumbo piston core samples, while samples from the remaining two core sites are from the Ocean Drilling Program. For the 26 piston or jumbo piston cores from the FSU AMGRF, we specifically targeted layers that had previously been identified as glacial diamict, or the sandy/gravel rich layers near the bottom of the piston cores, which are more likely to be tills (perhaps representing LGM deposition), and thus be sourced from the proximal rock substrate (see Pierce et al., 2011) (see Table 3 for description of samples). The Ocean Drilling Program provided the samples for one proximal site (ODP Site 1166) as well as the down-core samples from ODP Site 1165; from ODP Site 1165 we measured the U–Pb zircon ages from five IRD-rich samples (spanning 3.5 to 19 Ma in depositional age) that had already been analyzed for $^{40}Ar/^{39}Ar$ hornblende (Williams et al., 2010) and $^{40}Ar/^{39}Ar$ biotite (Pierce et al., 2011), in order to compare the inferred provenance based on the different thermochronometers. Depositional ages for the IRD-rich samples from ODP Site 1165 are discussed in Williams et al. (2010), but are primarily based on microfossil data.

4. U–Pb and $^{40}Ar/^{39}Ar$ analyses

Bulk till and glacial-marine sediment samples (~20 cm^3) were dried, weighed, disaggregated in deionized water, and washed through 63 μm sieves with deionized water. Subsequent sieving of dry samples was performed at 150 μm and 1 mm. Size fractions >63 μm (63–150 μm and 150 μm to 1 mm) were passed under a hand magnet and then passed through a Frantz magnetic separator at 0.8 Amp. with a side-slope of 20° and a front slope of 20°.

Hornblende and biotite grains were hand-picked from the magnetic 150 μm to 1 mm fraction and co-irradiated with the McClure Mountain hornblende (Mmhb) monitor standard either at the Cd-lined in-core facility (CLICIT) at the Oregon State rector, or (also with Cd shielding) at the U.S. Geological Survey (USGS) TRIGA reactor in Denver, CO. $^{40}Ar/^{39}Ar$ ages were obtained using single-step CO_2 laser fusion at the Lamont–Doherty Earth Observatory (L-DEO) argon geochronology lab (AGES: Argon Geochronology for the Earth Sciences). Calculated values include corrections for backgrounds based on frequent measurements of the blank, and for mass discrimination based on measurements of atmospheric argon. Corrections are made for nuclear interferences using values reported in Renne et al. (1998) for the OSU irradiations and in Dalrymple et al. (1981) for the USGS irradiations. J values used to correct for neutron flux were calculated using a value of 525 Ma and decay constants from Steiger and Jäger (1977) for the co-irradiated Mmhb-1 hornblende standard (Samson and Alexander, 1987).

The >150 μm non-magnetic fraction was sieved at 250 μm, and combined with the 63–150 μm non-magnetic fraction. The total 63–250 μm non-magnetic fraction was then passed through density separations in order to concentrate the zircons in the sample. The first density separation was performed with LST (lithium heteropolytungstates) at a density of 2.85 g/cm^3. The fraction >2.85 g/cm^3 was subsequently put through a density separation using MEI (Methylene Iodide) at a density of 3.3 g/cm^3. Zircons were handpicked from the >3.3 g/cm^3 fraction using a light microscope with polarizing lens capabilities. Zircon morphologies include both euhedral and rounded grain shapes, likely because they were recycled through one or more sedimentary cycles. Zircon grains were placed on double-sided tape mounted to glass slides. The grains were therefore not polished or imaged, so we cannot speak to the complexity of an individual grain; the point in this approach was to facilitate later analyses on U–Pb dated zircons, e.g., fission track and U–Th (He) dating.

U–Pb zircon analyses were performed at the University of Arizona's LaserChron facility, using laser ablation MC-ICP-MS. Corrections for instrumental bias were applied based on the measurement of a Sri Lankan zircon standard that was measured throughout the analytical session. The full procedure for this lab is reported on their website (https://sites.google.com/a/laserchron.org/laserchron/home/) and in Gehrels et al. (2006) and in Gehrels et al. (2008).

5. Results of the U–Pb and $^{40}Ar/^{39}Ar$ analyses

5.1. Results from shelf diamicts and core-top IRD (Cores 1–15, 17–28)

A total of 1915 U–Pb detrital zircons ages, 1169 $^{40}Ar/^{39}Ar$ hornblende ages, and 275 $^{40}Ar/^{39}Ar$ biotite ages were measured for

Table 3
Samples and analyses made for this study. Column headings from left to right: ID number assigned to cores for this study; name of the core from which the sample was taken; location of core in degrees latitude; location of core in degrees longitude; type of sample (SRL — sand rich layer; IRD — Ice rafted debris); depth of sample in the core; water depth of drill site; geographical sector assigned to core based on relative position of the core to East Antarctica; DML — Dronning Maud Land; PB — Prydz Bay; WL — Wilkes Land; Al — Adélie Land; GVL — George V Land; NVL — northern Victoria Land, study in which U–Pb zircon data was collected, number of zircon grains measured for U–Pb from sample, study in which $^{40}Ar/^{39}Ar$ hornblende data was collected, number of hornblende grains measured for $^{40}Ar/^{39}Ar$ from sample, study in which $^{40}Ar/^{39}Ar$ biotite data was collected, number of biotite grains measured for $^{40}Ar/^{39}Ar$ from sample, nm — not measured, vdf et al. (2008) — van de Flierdt et al. (2008).

								Studies associated with mineral analyses		Studies associated with mineral analyses		Studies associated with mineral analyses	
Site ID	Site name	Latitude (°)	Longitude (°)	Sample type	Sampling depth	Water depth (m)	Sector	Zircon	n	Hornblende	n	Biotite	n
1	IWSOE 68-11	−74.017	−54.75	SRL	11–18 cm	459	DML	This study	0	This study	67	This study	11
2	IWSOE 68 G8	−76.833	−40.917	SRL	10–17 cm	400	DML	This study	0	This study	6	This study	0
3	IWSOE 70 2-22-1	−77.533	−37.967	SRL	22–27 cm	1054	DML	This study	104	This study	71	This study	0
4	IWSOE 69 G17	−76.883	−32.833	SRL	158–162 cm	341	DML	This study	15	This study	96	This study	13
5	IWSOE69 G21	−72.8	−29.367	SRL	79–82 cm	3964	DML	This study	60	This study	55	This study	9
6	IWSOE 68 13	−75.45	−26.55	SRL	8–14 cm	507	DML	This study	42	This study	46	This study	17
7	IWSOE 70 03-11-03	−73.983	−23.65	SRL	228–230 cm	260	DML	This study	102	This study	20	This study	4
8	IO 1578-27	−72.408	−19.418	SRL	735.5–737	3274	DML	This study	20	This study	39	This study	19
9	IO 1578-28	−72.19	−15.305	SRL	235.5–237	58	DML	This study	77	This study	23	This study	8
10	IWSOE 70 3-17-2	−71.167	−12.367	SRL	55–59 cm	418	DML	This study	53	This study	97	This study	27
11	IO 1578-16	−70.612	−10.063	SRL	128–130 cm	366	DML	This study	77	This study	29	This study	22
12	IWSOE 70 3-18-1	−70.3	−6.807	SRL	31–33 cm	713	DML	This study	46	This study	46	This study	27
13	IO 1277-41	−69.998	−5.077	SRL	1161–1173 cm	1173	DML	This study	0	This study	23	This study	0
14	IO 1277-23	−67.897	14.58	SRL	887–889; 889–891	924	DML	This study	123	This study	57	This study	29
15	NBP01-01 JPC40	−67.176	65.737	diamict	2370 cm	750	PB	This study	100	This study	13	This study	25
16	ODP Site 1165B	−64.371	67.219	IRD	(see below)	3537	PB	This study	78	Williams et al. (2010)	167	Pierce et al. (2011)	145
17	NBP01-01 JPC34	−68.251	72.730	diamict	70, 292, 345	754	PB	This study	258	This study	318	This study	50
18	ODP Site 1166A	−67.696	74.787	diamict and fluvial	60, 80, 100 cm	475	PB	van de Flierdt et al. (2008)	232	van de Flierdt et al. (2008)	160	van de Flierdt et al. (2008)	16
19	NBP01-01 JPC25	−68.752	76.703	diamict	1305, 1405 cm	848	PB	This study	126	This study	37	This study	14
20	ELT49-30	−59.005	95.23	SRL	1698–1702 cm	4276	WL	This study	0	Pierce et al. (2011)	34	Pierce et al. (2011)	30
	ELT49-30 A			SRL	1276–1280 cm	4276		This study	0	This study	nm	This study	nm
21	ELT37-16	−63.97	127.447	SRL	231–235 cm	3840	WL	This study	0	Pierce et al. (2011)	63	Pierce et al. (2011)	57
	ELT37-16 A			SRL	228–233 cm	3840		This study	143	This study	38	This study	nm
22	ELT37-13	−64.672	132.977	SRL	113–120 cm	1333	WL	This study	33	Pierce et al. (2011)	47	Pierce et al. (2011)	29
	ELT37-13 A			SRL	112–117 cm	1333		This study	126	This study	44	This study	nm
23	ELT37-09	−65.552	141.095	SRL	140–144 cm	1308	AL	This study	10	Pierce et al. (2011)	45	Pierce et al. (2011)	28
	ELT37-09 A			SRL	137–139 cm	1308		This study	34	This study	16	Pierce et al. (2011)	59
24	NBP 01-01JPC11	−66.563	143.052	diamict	2305–2310 cm	870	AL	This study	10	Pierce et al. (2011)	15	Pierce et al. (2011)	14
	NBP 01-01JPC11			diamict	2370–2375 cm	870		This study	8	Pierce et al. (2011)	41	Pierce et al. (2011)	15
25	DF79-47	−66.667	148.733	SRL	563–567 cm	476	GVL	This study	17	Pierce et al. (2011)	46	Pierce et al. (2011)	10
	DF79-47 A			SRL	568.5–576 cm	476		This study	87	This study	18	This study	nm
26	DF80-34	−69.917	162.83	SRL	222–226 cm	805	NVL	This study	17	Pierce et al. (2011)	36	Pierce et al. (2011)	33
	DF80-34 A			SRL	213–222 cm	805		This study	71	This study	10	This study	nm
27	DF80-35	−70.017	166.417	SRL	269–273 cm	490	NVL	This study	0	Pierce et al. (2011)	21	Pierce et al. (2011)	23
	DF80-35 A			SRL	264–269 cm	490		This study	0	This study	11	This study	nm
28	DF80-20	−69.783	163.683	SRL	160–164 cm	475	NVL	This study	0	Pierce et al. (2011)	8	Pierce et al. (2011)	35
	DF80-20 A			SRL	152–160 cm	475		This study	0	This study	nm	This study	nm
Downcore record ODP Site 1165B													
		−64.371	67.219				PB						
16	ODP Site 1165	3.5 Ma		IRD	1165B-4H-6 (80)			This study	10	Williams et al. (2010)	40	Pierce et al. (2011)	41
16	ODP Site 1165	4.65 Ma		IRD	1165B-6H-1 (70)			This study	3	Williams et al. (2010)	32	Pierce et al. (2011)	28
16	ODP Site 1165	7 Ma		IRD	1165B-10H-2 (35)			This study	31	Williams et al. (2010)	31	Pierce et al. (2011)	39
16	ODP Site 1165	19 Ma		IRD	1165C-10R-3 (120)			This study	13	Williams et al. (2010)	23	Pierce et al. (2011)	37
16	ODP Site 1165	4.65 Ma		IRD	1165B 6H-1 100/102			This study	21	Williams et al. (2010)	41	Pierce et al. (2011)	–

this study, adding to 683 $^{40}Ar/^{39}Ar$ hornblende ages, 494 $^{40}Ar/^{39}Ar$ biotite ages, and 232 U–Pb detrital zircon ages from previous studies (van de Flierdt et al., 2008; Williams et al., 2010; Pierce et al., 2011) for a total of 2147 U–Pb detrital zircon ages, 1863 $^{40}Ar/^{39}Ar$ hornblende ages, and 769 $^{40}Ar/^{39}Ar$ biotite ages (see Table 3). Twenty of the 27 piston jumbo core samples have measurements made on all three of the mineral systems, while in six samples we did not find any zircons, and in three samples we did not find any biotite (see Appendix A for U–Pb zircon data listed by sample location, Appendix B for $^{40}Ar/^{39}Ar$ hornblende data listed by sample location, Appendix C for biotite data listed by sample location, Appendix D for data grouped by geographic sector, and Appendix E for stacked histograms of each system (U–Pb zircon, $^{40}Ar/^{39}Ar$ hornblende, $^{40}Ar/^{39}Ar$ biotite) by individual core site).

Fig. 3a–d shows stacked histograms of each system (U–Pb zircon, $^{40}Ar/^{39}Ar$ hornblende, $^{40}Ar/^{39}Ar$ biotite) by geographic sector (A) Dronning Maud Land (DML), (B) Prydz Bay (PB), (C) Wilkes Land (WL) and (D) Adélie/George V/northern Victoria Land (AL/GVL/NVL). ISOPLOT/EX (Ludwig, 2003) was used for determining the peak ages in the detrital data sets. For comparison, we have included a histogram of on-land U–Pb zircon ages from each sector, taken from compilations in Veevers (2012) and Veevers and Saeed (2011).

5.1.1. Weddell and Dronning Maud Land sector (Cores 1–14, 60°W to 15°E)

Detrital zircon U–Pb ages from the core sites in the Dronning Maud Land (DML) sector show dominant populations of 500–600 Ma (peak age 520 Ma) and 1000–1200 Ma (peak ages ~1068 and ~1104), with additional small populations at ~108 Ma, ~180 Ma, ~760 Ma, ~1796 Ma ~2588 Ma and ~2736 Ma. $^{40}Ar/^{39}Ar$ hornblende ages show dominant populations of 440–540 Ma (peak age ~494 Ma), 960–1100 Ma (peak age ~1056 Ma), with smaller populations of ~92 Ma, ~174 Ma, ~1236 Ma, ~2890 Ma and ~3080 Ma. $^{40}Ar/^{39}Ar$ biotite ages show dominant populations of 400–500 Ma (peak age ~451 Ma) and 900–1100 Ma (peak ages ~976 Ma and ~1011 Ma), with smaller populations of ~211 Ma and ~2550 Ma, ~2602 Ma and ~2644 Ma (Fig. 3a).

5.1.2. Prydz Bay sector (Cores 15, 17–19, 60°E to 80°E)

Detrital zircon U–Pb ages from cores in the Prydz Bay (PB) sector show dominant populations of 500–600 Ma (peak age 540 Ma) and 840–1040 Ma (peak age 932 Ma), with a continuum of zircon ages between these two peaks and a smaller population of 680 to 720 Ma (peak age ~698 Ma), and minor populations of ~2064 Ma and ~2766 Ma. $^{40}Ar/^{39}Ar$ hornblende ages show dominant populations of 480–540 Ma (peak age ~500 Ma) and a minor population of 580–640 Ma (peak age ~628 Ma). $^{40}Ar/^{39}Ar$ biotite ages show a dominant population of 480–540 Ma (peak age ~500 Ma) (Fig. 3b).

5.1.3. Wilkes Land sector (Cores 20–22, 90°E to 135°E)

Detrital zircon U–Pb ages from cores in the Wilkes Land (WL) sector show dominant populations of 1100–1200 Ma (peak ~1150 Ma) and 1480–1620 Ma (peak age ~1562 Ma). $^{40}Ar/^{39}Ar$ hornblende ages show a dominant population of 1100–1200 Ma (peak age ~1152 Ma), and a small population 1440 to 1500 Ma (peak age ~1494 Ma). $^{40}Ar/^{39}Ar$ biotite ages show a dominant population of 1080–1160 Ma (peak age ~1120 Ma) and a small population of 400–500 Ma (peak age ~440) (Fig. 3c).

5.1.4. Adélie Land/George V Land/northern Victoria Land (Cores 23–28, 140°E to 165°E)

Detrital zircon U–Pb ages from all cores in the Adélie/George V/northern Victoria Land (AL/GVL/NVL) sector show dominant populations of 480–620 Ma (peak ages ~502 and 579 Ma) and 380–400 Ma (peak age ~389 Ma), with small populations of ~1057 Ma, ~1235 Ma, ~1610 Ma, ~1723 Ma, ~1795 Ma, ~2455 Ma and ~2717 Ma. $^{40}Ar/^{39}Ar$ hornblende ages show dominant populations of 480 to 520 Ma (peak age ~ 493 Ma) and 0–20 Ma (peak age ~ 3 Ma), with small populations of ~1480 Ma, 1608 Ma and 1715 Ma. $^{40}Ar/^{39}Ar$ biotite ages show dominant populations of 340–440 Ma (peak age ~369 Ma) and 460–540 Ma (peak age ~ 494 Ma), with small populations of ~105 and ~1626 Ma (Fig. 3d).

5.2. ODP Site 1165 — downcore results (Core 16)

Sixty-seven zircons were found in five layers previously studied from ODP Site 1165. For $^{40}Ar/^{39}Ar$ hornblende ages (167 grains; Williams et al., 2010) and $^{40}Ar/^{39}Ar$ biotite ages (145 grains; (Pierce et al., 2011)). Fig. 4 shows stacked histograms of each mineral type for each of the IRD layers.

Three of the five layers yielded few U–Pb zircon analyses (n = 3 to 13), and a mix of ~500 Ma and 1000–1200 Ma grains (3.0 Ma, first 4.65 Ma, and 19.0 Ma; Fig. 4). The remaining two layers both contain more robust ~500–600 Myr and 1100–1200 Myr age populations, with the latter being more prominent in the layer deposited 4.65 Ma, while the 7.0 Ma layer contains roughly equal proportions of both populations.

6. Discussion and comparison of thermochronometers

6.1. Relationship between detrital ages and on-land geology

While our new detrital age populations are in general agreement with major known tectonothermal events on land, the results also reveal age populations that have not previously been reported from onshore studies. These 'unexpected' age populations reflect either a bias in the types of measurements made from on-land samples (e.g., U–Pb zircon ages dominate the on-land record) or the presence of ice-covered terranes that are not accessible for direct study today, and will be discussed below in more detail. We will discuss our new data by geographic sector, starting with a comparison to known source rock ages (from old to young) (Fig. 5a, b and c) (see Appendix F for a table of on-land ages and references to published geological studies) and followed by new and interesting age populations that have not previously been described.

6.1.1. Dronning Maud Land Sector (Cores 1–14, 60° W to 15°E)

6.1.1.1. Results consistent with onshore outcrop data

6.1.1.1.1. Archean ages. Overall, Archean zircons (n = 30) are scattered in the 2500–3700 Ma range, with minor populations of ~2588 Ma and ~2736 Ma. Marschall et al. (2010) measured U–Pb ages in zircons recovered from the Annandagstoppane granite, which outcrops in the Grunehoga Craton, and determined the crystallization age of the granite to be 3067 ± 8 Ma, with evidence of inherited zircon ages ranging from 3175 ± 8 to 3433 ± 7 Ma. The low abundance of zircon in this granite, in addition to the lack of sorting during ice transport, is likely why there is no distinct population of U–Pb ages in the zircons measured in these cores. The spread of ages between 3100 Ma and 3700 Ma, however, is consistent with the inherited U–Pb zircon ages measured in the Annandagstoppane granite by Marschall et al. (2010), and with ages of tectono-magmatic events measured in the Kaapvaal craton, thus lending support to the conclusion of Marschall et al. (2010) that the Grunehogna craton was an extension of Africa's Kaapvaal craton.

6.1.1.1.2. Grenvillian activity. Based on previous data, Fitzsimons (2000) divided Grenvillian U–Pb zircon ages in the DML area into those older than 1100 Ma, reflecting igneous crystallization of orthogneiss and metavolcanic precursors, and those 1030–1090 Ma, reflecting high-grade Grenville-aged tectonism. Grenville-aged populations appear in each of the mineral systems, with peak ages of ~1068 Ma ~1104 Ma (U–Pb zircon), ~1056 Ma ($^{40}Ar/^{39}Ar$ hornblende) and ~1011 Ma and ~976 Ma ($^{40}Ar/^{39}Ar$ biotite).

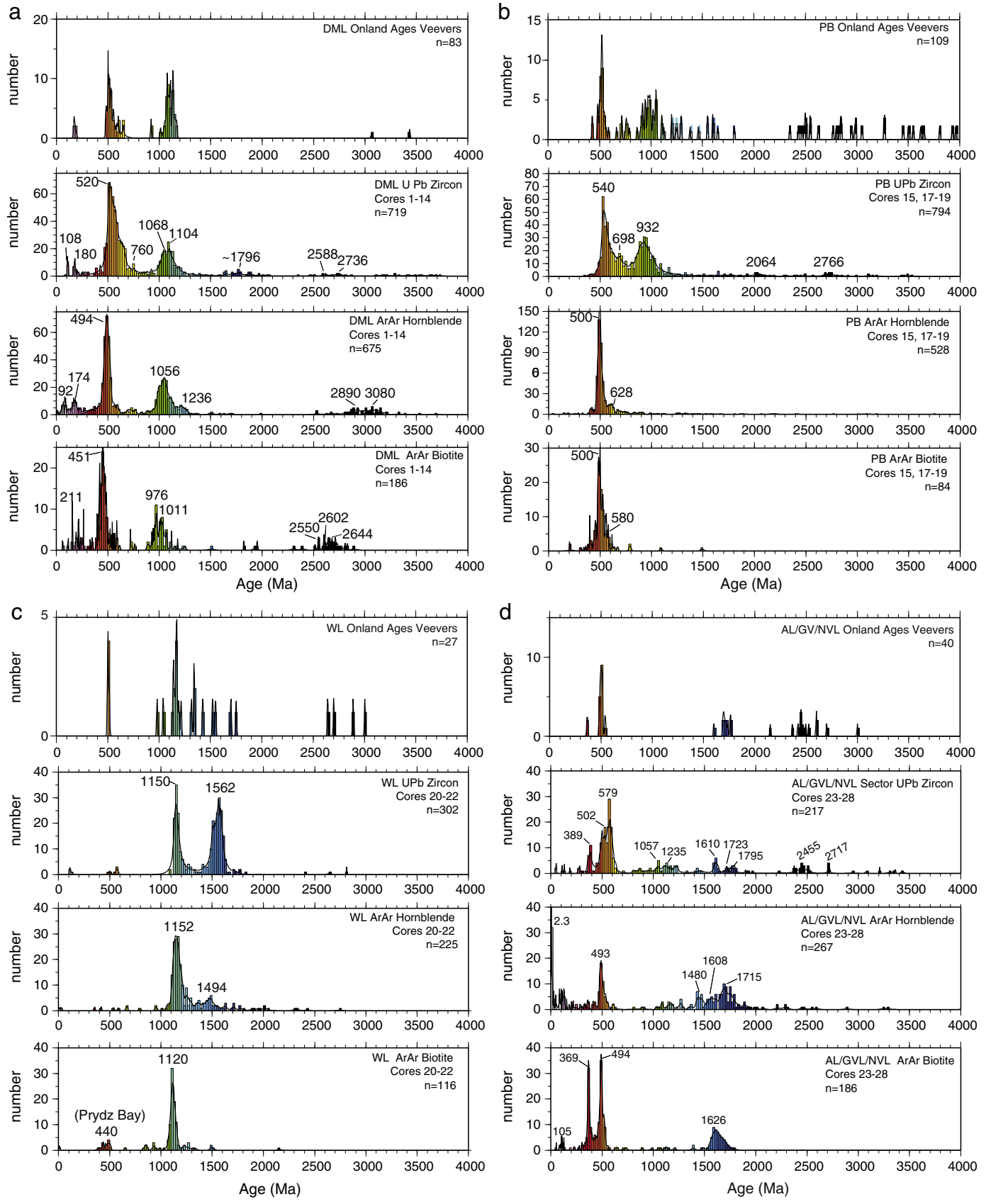

Fig. 3. Histograms (20 Myr bins) and probability plots of detrital U–Pb zircon, $^{40}Ar/^{39}Ar$ hornblende and $^{40}Ar/^{39}Ar$ biotite ages by geographic sector compared to a histogram (20 Myr bin) and probability plot of on-land ages taken from the compilation of Veevers (2012) and Veevers and Saeed (2011). The color scale used here is the same as that used in Figs. 4 and 5A–C, and corresponds to 100 Myr increments of time. a) DML — Dronning Maud Land b) PB — Prydz Bay c) WL — Wilkes Land and d) AL / GVL / NVL — Adélie Land, George V Land and northern Victoria Land. (For the color version of this figure, the reader is referred to the web version of this article.)

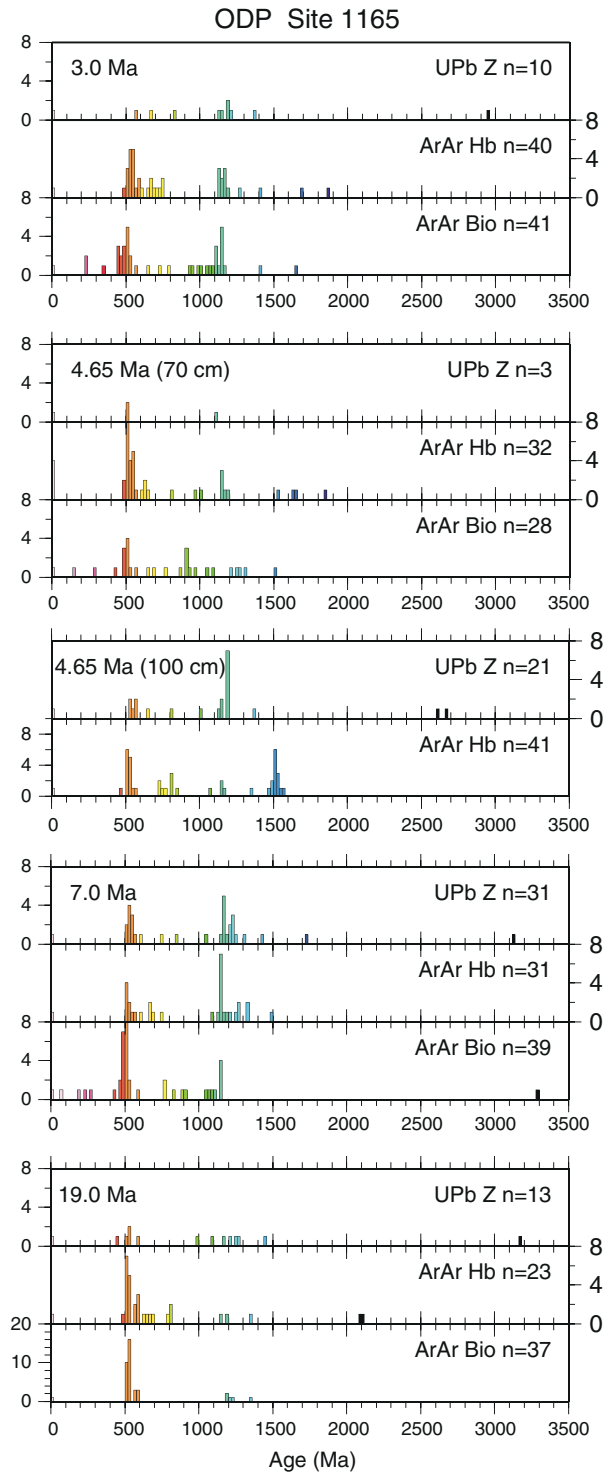

Fig. 4. Stacked histograms (20 Myr bins) showing the U–Pb zircon (this study), $^{40}Ar/^{39}Ar$ hornblende (Williams et al., 2010) and $^{40}Ar/^{39}Ar$ biotite (Pierce et al., 2011) ages from the IRD recovered from ODP Site 1165 record. The depositional age of each layer is in the top left corner of each set of histograms. The color scale used here is the same as that used in Figs. 3 and 5A–C, and corresponds to 100 Myr increments of time. (For the color version of this figure, the reader is referred to the web version of this article.)

The range of Grenvillian ages we have measured is consistent with Fitzsimons (2000) survey, as well as with measured on-land ages that fall in the 1030–1090 Ma range (Harris et al., 1995; Jacobs et al., 1996, 2003a, 2003b, 2003c; Board et al., 2005; Bisnath et al., 2006; Jacobs et al., 2008) and the greater than 1100 Ma range (Arndt et al., 1991; Harris et al., 1995; Gose et al., 1997; Jackson, 1999; Board et al., 2005; Bisnath et al., 2006; Flowerdew et al., 2012). Both the ~1104 Ma and 1068 Ma detrital zircon U–Pb peaks are consistent with U–Pb zircon ages of 1104 ± 8 and 1070 Ma measured by Bisnath et al. (2006) in Gjelsvikfjella (~3°W). The Grenvillian ages found in Core 1 (Western Weddell Sea, Fig. 5a–c) likely reflect sourcing from the Haag Nunatak area, which has been shown to contain Grenvillian ages ~1000–1180 Ma Rb–Sr whole rock ages (Millar and Pankhurst, 1987), and 991–1031 K–Ar hornblende and biotite ages (Clarkson and Brook, 1977).

6.1.1.1.3. Pan-African/Ross orogeny. The ~500 Ma populations found in each of the detrital thermochronometers from this area likely reflect a mix of Pan-African and Ross signatures from the bedrock source. Reconstructions of Gondwana (e.g., Harley and Kelly, 2007; Kleinschmidt, 2007; Fig. 1), project the Ross orogen all the way from northern Victoria Land through to Coats Land, in addition to having Pan-African rocks potentially projected from Enderby Land along a continuation of the Lützow–Holm Belt (to the Coats Land area as well (see Fig. 1)). Given the close temporal overlap between these orogenies, we may not be able to use detrital mineral grain age populations to tease apart the two orogenies. However, based on the reconstructions mentioned above, we tentatively assign the ~500 Ma grain in Cores 1–3 as having a 'Ross' orogen source, while the ~500 Ma grains in Cores 5–14 are assigned a 'Pan-African' source. Additionally, there is an older tail age in the Pan-African ages, and less so than in the Ross consistent with the findings of Pierce et al. (2011).

Pan-African/Ross populations appear in each of the thermochronometeric ages, with peak ages of ~520 Ma, ~494 Ma, and ~451 Ma for detrital U–Pb zircon, $^{40}Ar/^{39}$ hornblende and $^{40}Ar/^{39}Ar$ biotite, respectively, and are consistent with Pan-African ages measured on-land in zircons (Mikhalsky et al., 1997; Harris, 1999; Zeh et al., 1999; Jacobs et al., 2003a, 2003b, 2003c; Paulsson and Austrheim, 2003; Curtis et al., 2004; Board et al., 2005; Bisnath et al., 2006; Flowerdew et al., 2012), with only a few $^{40}Ar/^{39}Ar$ hornblende (Jacobs et al., 1995, 1996, 1997; Board et al., 2005) and one $^{40}Ar/^{39}Ar$ biotite age (Board et al., 2005) falling in this range.

The pattern that emerges from the age distribution in the thermochronometers in this area reflects Ross and Pan-African overprinting of Grenville-aged rocks in some areas but not others. Core 4, which consists purely of Grenvillian age populations in each of the thermochronometers, is located adjacent to the Bertrab–Littlewood–Moltke nunataks (see Fig. 5), which have U–Pb zircon ages of 1000–1100 Ma (Gose et al., 1997; Storey et al., 2004), and which did not undergo any metamorphism during the Pan-African/Ross orogenies. To the east of Core 4, Cores 5 and 6 contain bimodal populations of Pan-African/Ross and Grenvillian ages in each of the chronometers. To the east of Core 6, and of the cores that contain all thermochronometers, Cores 7, 8, 11, 12 and 14 contain Grenvillian and Pan-African U–Pb age populations, while the $^{40}Ar/^{39}Ar$ hornblende and biotite age populations are dominated by Pan-African ages, with few to no Grenvillian ages (Fig. 5, Table 4); this finding argues for significant resetting during the Pan-African orogenyin locations onshore of these core sites. These results are consistent with the interpretation of Jacobs and Thomas (2004), who show that Coats Land was unaffected by Pan-African overprinting due to lateral escape tectonics.

6.1.1.1.4. Jurassic rifting and younger ages. Grains less than 200 Ma in age are present in the detrital zircon U–Pb and $^{40}Ar/^{39}Ar$ hornblende and biotite populations, though as a very small percentage (Figs. 3A, 5A–C). Zircons and hornblendes both contain populations of ~180 and ~100 Ma, while the biotite ages are more scattered from 160 to 211 Ma. The small population of ~100 Ma and younger ages are consistent with measured on-land ages south of the Ronne–Filchner Ice Shelf (Gose et al., 1997; Vaughan and Storey, 2000; Flowerdew et al., 2012), and are characteristic of the Antarctic Peninsula and West Antarctica (indeed, these ages are predominantly found in the cores located closest to the Antarctic Peninsula (Roy et al., 2007b)).

The small age peak at ~180 Ma and ~174 Ma in the detrital zircon U–Pb and $^{40}Ar/^{39}Ar$ hornblende ages, respectively, are from cores located off the coast of Coats Land; these likely reflect sourcing from the Dufek–Ferrar–Karoo volcanic rocks. U–Pb zircon dates of ~183 Ma have been measured in the Sonora Bluffs and surrounding area (Minor and Muakas, 1997; Flowerdew et al., 2012), while slightly younger $^{40}Ar/^{39}Ar$ hornblende ages of 179 Ma and 175 Ma have been measured in the same areas (Fig. 5a–c). Hornblendes with these ages are additionally found farther along the coast to the east (Cores 7–9), and reflect sourcing from the extension of the Karoo flood basalts in the Vestfjella region, which have whole rock K–Ar ages of 160–230 Ma (Furnes and Mitchell, 1978; Furnes et al., 1987; Peters et al., 1991), and a plagioclase K–Ar age of 180 Ma (Peters et al., 1991). $^{40}Ar/^{39}Ar$ ages measured on the lavas in adjacent Kirwanveggan have an age of 183 ± 1 Ma (Duncan et al., 1997), consistent with ages further to the south in Coats Land, while $^{40}Ar/^{39}Ar$ ages from the Ferrar dolerite in Transantarctic Mountains yield an age of ~176 Ma (Flemming et al., 1995).

6.1.1.2. Novel and previously un-described age populations

6.1.1.2.1. Archean $^{40}Ar/^{39}Ar$ hornblende and biotite ages. Archean grains comprise a small population of the total analyses made on cores off the coast of Dronning Maud Land. The majority (76%) of the Archean grains found in the cores off the coast of DML are either hornblende or biotite, and are from Core sites 10–12, located directly offshore of the Archean Grunehoga craton (Fig. 5b, c). The Grunehoga craton is a continuation of South Africa's Kalahari craton in East Antarctica (e.g., Marschall et al. (2010), see Fig. 1), and, though only exposed in a few nunataks, has been interpreted to extend from ~2° to 15°W, along ~72°S based on geophysical surveying (Jacobs et al., 1996).

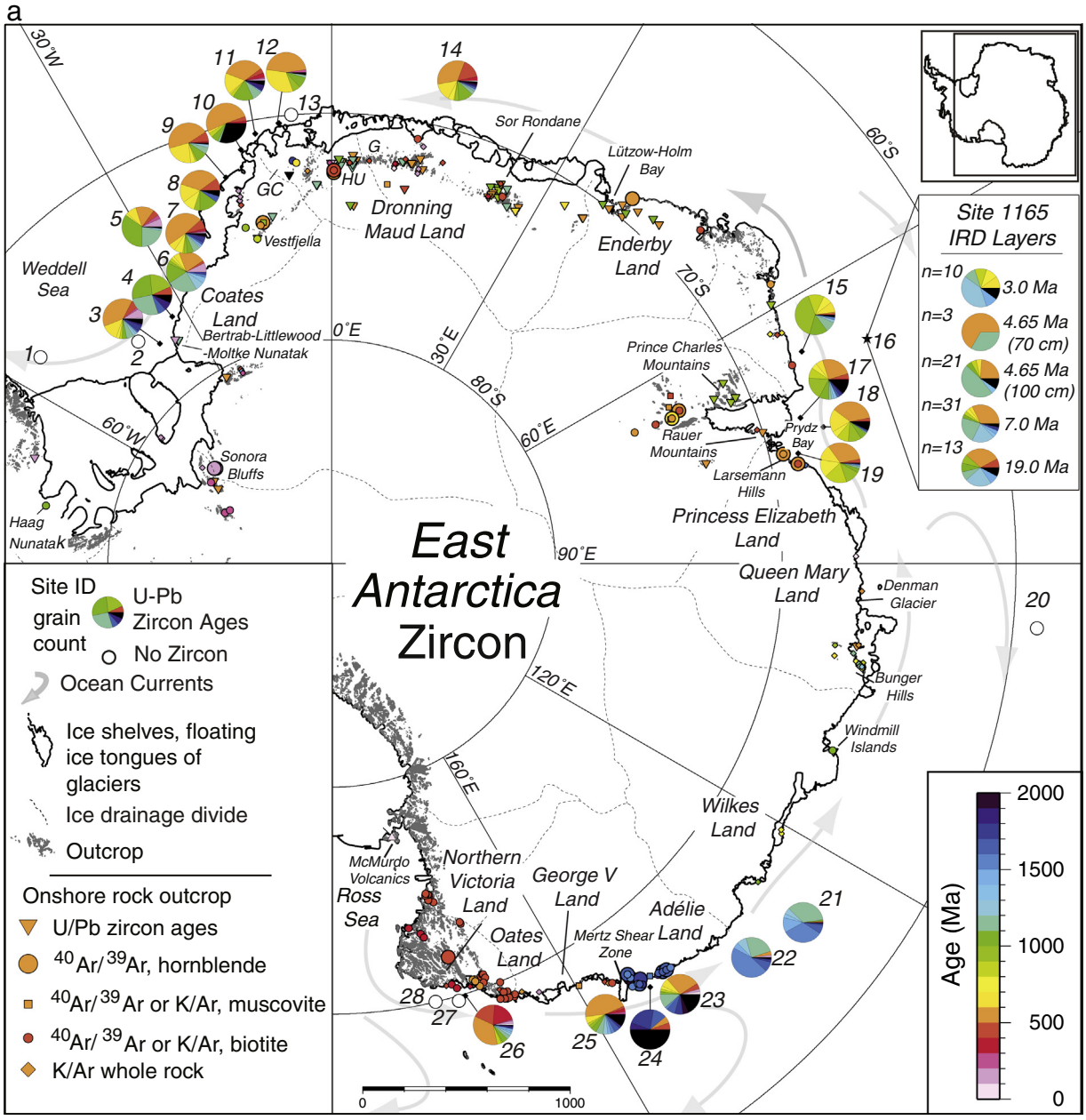

Fig. 5. Maps of East Antarctica with pie charts showing the distribution of thermochronologic ages by site location and mineral type, the down-core ODP Site 1165 record of IRD, and known onshore ages (see Appendix F for onshore thermochronologic age references). The color scale used here is the same as that used in Figs. 3 and 4, and corresponds to 100 Myr increments of time. a) Pie charts displaying U–Pb zircon results b) Pie charts displaying $^{40}Ar/^{39}Ar$ hornblende results c) Pie charts displaying $^{40}Ar/^{39}Ar$ biotite results. GC — Grunehogna Craton, G — Gjelsvifjella, H — Haag Nunatak, HU — H.U. Sverdrupfjella, K — Kirwanveggan. (For the color version of this figure, the reader is referred to the web version of this article.)

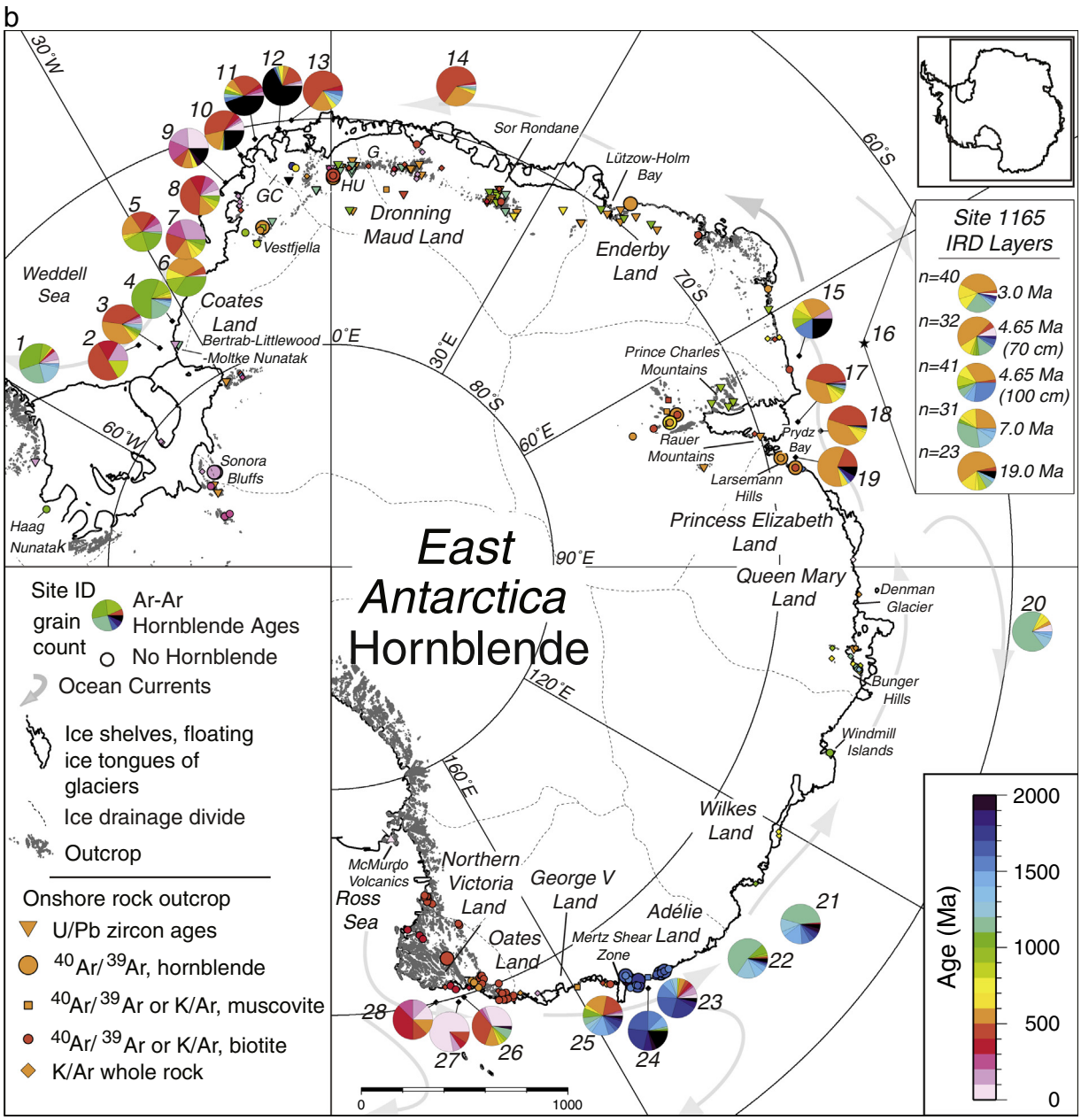

Fig. 5 (*continued*).

Archean hornblendes (n = 71) form a broad population of ~2800–3200 Ma. The older ages in this population are consistent with the U–Pb zircon age of 3067 ± 8 Ma obtained by Marschall et al. (2010) for the crystallization age of the Annandagstoppane granite. However, no hornblende is reported in the petrographic descriptions of the Annandagstoppane granite (Barton et al., 1987). We therefore suggest that additional hornblende-rich Archean basement lithologies may be obscured by ice in the Dronning Maud Land sector. This proposition is supported by the occurrence of a ~2900 Ma $^{40}Ar/^{39}Ar$ hornblende population, which cannot be tied to known ages measured in outcrops.

Archean biotite grains contain a population of ~2602 to 2644 Ma, indicating the Grunehoga craton as a source, and indeed the Annandagstoppane granite contains accessory (<5%) amounts of biotite (Barton et al., 1987). These younger $^{40}Ar/^{39}Ar$ biotite ages may reflect cooling following a tectonothermal event at 2800 Ma (Barton et al., 1987). However, Barton et al. (1987) also report on an ~1200 Ma event (intrusion of the Annandagstoppane gabbro), which reset the Rb–Sr biotite ages in the Annandagstoppane granite. It may be that with these biotite grains, we are tapping a previously unstudied part of the Grunehoga craton, containing biotites that were either undisturbed or only partially disturbed during Grenvillian or Pan-African metamorphism. The relatively small range of ages of this population leads us to favor a lack of post-Archean disturbance of the source.

6.1.1.2.2. ~1200–1300 Ma $^{40}Ar/^{39}Ar$ hornblende ages. Core 1, in the western Weddell Sea, contains a significant 1200–1300 Ma population in the $^{40}Ar/^{39}Ar$ hornblende ages, which are significantly older than the detrital U–Pb zircon ages from this sector. While there are no reported 1200–1300 Ma $^{40}Ar/^{39}Ar$ hornblende ages from outcrops in DML, these grains are likely sourced from the ice-covered continuation of the Natal Metamorphic Province (South Africa), which is this area of

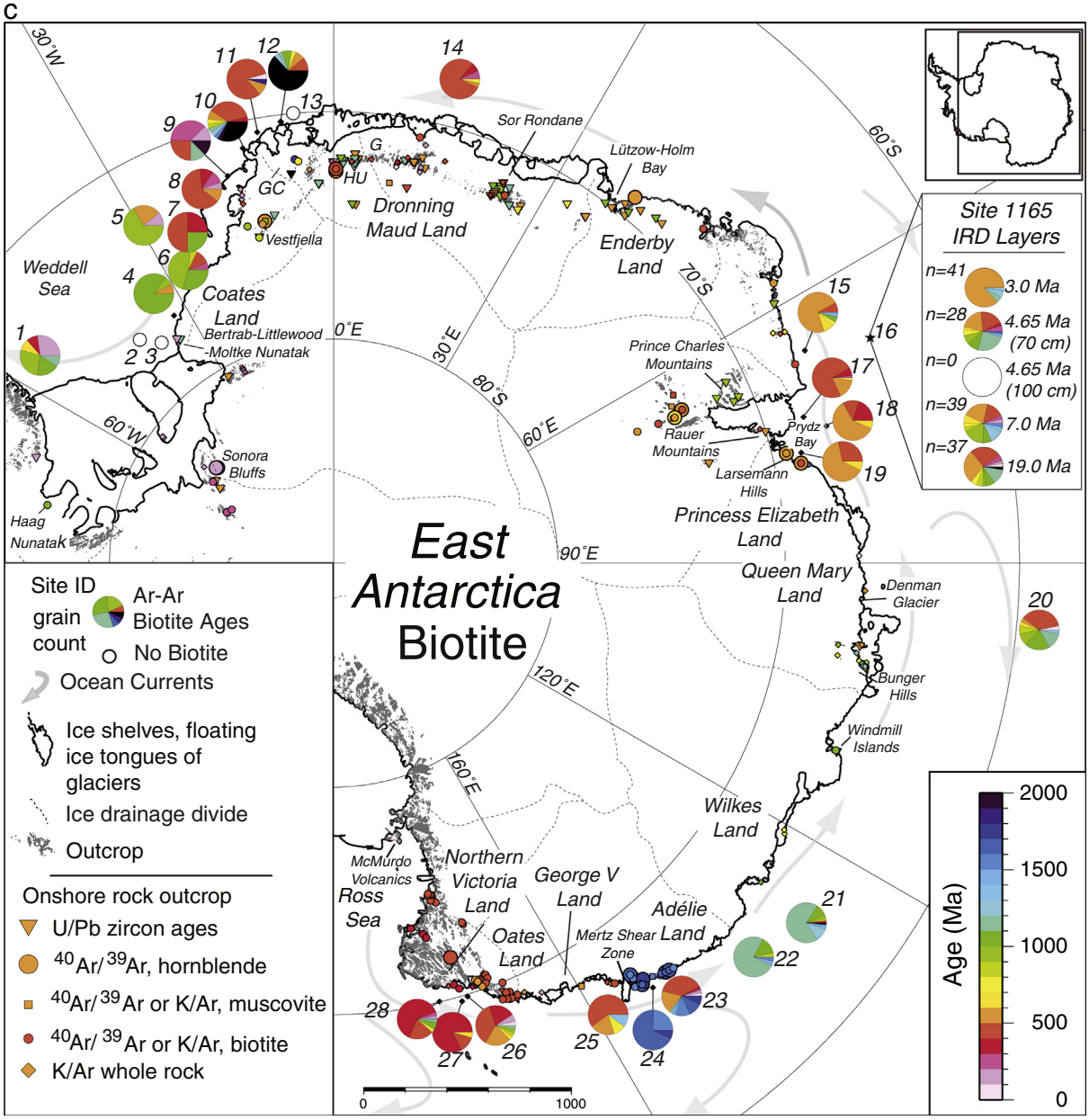

Fig. 5 (*continued*).

East Antarctica's conjugate margin in South Africa. The Quaha Formation specifically has U–Pb zircon ages between 1235 ± 9 and 1207 ± 10 Ma (Thomas et al., 1999).

6.1.1.2.3. Grenvillian $^{40}Ar/^{39}Ar$ hornblende and biotite ages. While there are no reported Grenvillian $^{40}Ar/^{39}Ar$ hornblende ages from outcrops in DML, Grenvillian (~991–1031) K–Ar dates for hornblende and biotite from the Haag Nunatak (West Antarctica) have been reported (Clarkson and Brook, 1977). The presence of Grenvillian-aged detrital $^{40}Ar/^{39}Ar$ hornblende populations in the marine sediment samples (primarily Cores 1, 4, 5 and 6; see Fig. 5b) indicates that hornblendes with this age are indeed present in DML. Similarly, only one Grenvillian $^{40}Ar/^{39}Ar$ biotite age (974 Ma; Jacobs et al. (1995)) is reported from outcrops in DML, though these ages are found in many of the core sites offshore DML (Fig. 5a–c). The presence of Grenvillian ages likely reflects sourcing from areas that were not overprinted by Pan-African activity, as a result of escape tectonics (Jacobs and Thomas, 2004), but which are currently obscured by the ice sheet.

6.1.2. Prydz Bay (Cores 15, 17–19, 60°E to 80°E)

6.1.2.1. Results consistent with onshore outcrop data

6.1.2.1.1. Grenvillian activity. The ~932 Ma detrital zircon U–Pb ages agree well with Grenvillian ages of 900–990 Ma attributed to this area by Fitzsimons (2000), as well as additional on-land studies (Kinny et al., 1993; Boger et al., 2000; Carson et al., 2000; Liu et al., 2007).

6.1.2.1.2. ~700 Ma event?. The presence of small ~698 Ma and ~628 Ma populations in the detrital zircons, and hornblendes, respectively, may reflect a possible ~700 Ma metamorphic event (and subsequent cooling) recorded in the Prince Charles Mountains (Tong et al., 2002).

6.1.2.1.3. Pan-African orogeny. The dominant detrital zircon U–Pb (~540 Ma) and $^{40}Ar/^{39}Ar$ hornblende and biotite (~500) age populations are consistent with the pervasive Pan-African (500–650 Ma) overprinting found in outcrops in the area (Stüwe and Oliver, 1989; Zhao et al., 1992; Fitzsimons et al., 1997; Zhao et al., 1997; Tong et al., 1998; Tong et al., 2002; Meert, 2003; Veevers, 2003, 2004; Liu et al., 2006, 2007; Wang et al., 2007; Veevers and Saeed, 2011; Veevers, 2012), as well as in Eocene fluvial sediments from ODP Site 1166 (van de Flierdt et al., 2008) and early Oligocene through Pliocene glacial-marine sediments from ODP Site 739 (Tochilin et al., 2012). Onshore $^{40}Ar/^{39}Ar$ dates only show ages consistent with Pan-African over-printing, and complete resetting, of hornblende and biotite during the Pan-African orogeny, with no Grenville-aged hornblende or biotite ages reported (Tong, 2004; Phillips et al., 2007; Wilson et al., 2007).

6.1.2.2. Novel and previously un-described age populations. Overall, detrital age populations from the Prydz Bay sector are in general agreement with onshore ages, and no unexpected populations were discovered. As the Prydz Bay area is one of the best-exposed terrains within East Antarctica, this finding lends additional support to the value of using detrital mineral grain ages in marine sediments to infer onshore (and sub-ice) geology.

6.1.3. Wilkes Land (Cores 20–22, 90°E to 135°E)

6.1.3.1. Results consistent with onshore outcrop data. The Wilkes Land coastline has very few accessible outcrops ((Tingey, 1991; Anderson, 1999); Figs. 2, 5A–C), with onshore thermochronologic measurements coming only from the Denman Glacier/Bunger Hills (Black et al., 1992; Fitzsimons, 2000), and the Windmill Islands (Post et al., 1996; Post, 2000; Möller et al., 2002; Fitzsimons, 2003) (Figs. 2, 5A–C). Detrital $^{40}Ar/^{39}Ar$ hornblende and biotite ages from this sector are dominated by Grenvillian ages (1152 Ma and 1120 Ma peak ages, respectively), while the detrital zircon U–Pb ages show two peaks at ~1150 Ma and ~1562 Ma (discussed above, Section 6.1.3.1). The Grenvillian ages agree well with reports from Fitzsimons (2000) and Sheraton et al. (1992, 1993), which conclude that high-grade metamorphism affected the Wilkes Land sector from 1130 to 1200 Ma. Given the dearth of outcrops along this part of East Antarctica, more studies utilizing this approach and sampling proximal glacial-marine sediments would surely yield further important clues about the geology along this margin. The small 400–500 Ma population seen in the $^{40}Ar/^{39}Ar$ hornblende ages comes from Core 20, located offshore of the boundary between Wilkes Land and the Pan-African overprinting seen in the Prydz Bay region, and so reflects this boundary location and is not seen in the other cores from this sector.

6.1.3.2. Novel and previously un-described age populations

6.1.3.2.1. ~1562 Ma population of U–Pb zircons. Our detrital U–Pb zircon results from Cores 21 and 22 show that half of the zircon population falls in the 1500–1600 Ma range, with a peak age of ~1562 Ma. There are no outcrops directly onshore from these core locations. However, just to the west of Wilkes Land, outcrops in the Bunger Hills area (~100°E) consist of granulite-facies metamorphic rocks. The emplacement of granodioritic orthogneisses in the Bunger Hills areas is dated at ~1521 ± 29 Ma (Thomas Island) and ~1700 Ma (southwest Bunger Hills) by U–Pb zircon ages (Sheraton et al., 1992, 1993). Additionally, Fitzsimons (2003) reported on a 1500–1600 Ma population of inherited U–Pb zircon ages from a psammitic gneiss in the Windmill Island area. The presence of ~1562 Ma U–Pb zircon ages from Cores 21 and 22 could require an extension of the granodioritic orthogneiss, or associated units, over 1000 km to the east. However, without a better spatial coverage of detrital U–Pb zircon analyses from marine sediment cores, this is entirely speculative. Veevers and Saeed (2011) measured detrital U–Pb zircon ages from Miocene–Oligocene samples recovered at DSDP Site 269 (Fig. 5), off the coast of East Antarctica near the boundary between Wilkes and Adélie Land, and just to the west of Core 21; their analyses revealed two minor peaks at ~1166 Ma and ~1570 Ma. These two age peaks are consistent with our U–Pb zircon ages. Veevers and Saeed (2011) attribute these to 'ice covered gaps' in the data available from outcrops.

Additionally, the ~1560 Ma population in the U–Pb zircon ages could represent continuation of the south Australian Kararan orogen (1570 to 1540 Ma) into East Antarctica. Boger (2011) discusses the likely continuation of accreted domains (Nawa and Musgrave) under the East Antarctic ice sheet, between 115° to 140°E, and our sampling sites which contain this age population are located at ~127°E and ~133°E.

6.1.3.2.2. ~1494 Ma population of $^{40}Ar/^{39}Ar$ hornblendes. There is a small $^{40}Ar/^{39}Ar$ hornblende peak at ~1494 Ma (mostly found in Core 21), which could be associated with cooling following the older ~1560 Ma event recorded by the U–Pb zircon ages. Indeed, the granodioritic gneiss does contain hornblende. While this would require the hornblende to have withstood resetting during the metamorphism associated with Grenvillian activity in this sector (see 6.1.3.2), this may be possible if they were sourced from far inside the East Antarctic craton. Alternatively, these grains could represent incomplete resetting during Grenvillian activity. Further work with these samples, such as $^{40}Ar/^{39}Ar$ step-heating experiments would help to test this.

6.1.4. Adélie Land/George V Land/northern Victoria Land (Cores 23–28, 140°E to 165°E)

6.1.4.1. Results consistent with onshore outcrop data. Two high-grade thermal events occurred in the Adélie craton ~1700 and ~2500 Ma (Peucat et al., 1999; Di Vincenzo et al., 2007; Ménot et al., 2007). Notably, there are no Grenvillian or Ross ages from outcrops in Adélie Land, making it one of the few areas in East Antarctica where the Archean craton is preserved in nearly pristine condition, while northern Victoria Land, Oates Land and George V Land to the east of the Mertz shear zone are dominated by Ross orogen (550–480 Ma) ages (Black and Sheraton, 1990; Tingey, 1991; Tessensohn and Henjes-Kunst, 2005; Di Vincenzo et al., 2007; Tribuzio et al., 2008) (Fig. 5a–c).

6.1.4.1.1. Archean and Proterozoic terranes. Detrital zircon U–Pb ages from the Adélie/George V/northern Victoria Land sector show age populations of ~2455 to ~2717 Ma, consistent with onshore ages (Oliver and Fanning, 1997; Peucat et al., 1999; Fitzsimons, 2003; Ménot et al., 2007; Duclaux et al., 2008; Veevers and Saeed, 2011) and offshore ages from marine sediments (Goodge and Fanning, 2010).

There is a broad 1600–1800 Ma population in the U–Pb zircon, $^{40}Ar/^{39}Ar$ hornblende and $^{40}Ar/^{39}Ar$ biotite ages. Detrital zircon U–Pb ages within this range show small peaks at ~1795 Ma, ~1723 Ma, and ~1610 Ma, which are also consistent with onshore ages in Adélie Land. Ménot et al. (2007) reported U–Pb zircon ages of ~1600 Ma in western Adélie Land, while Peucat et al. (1999) obtained U–Pb ages of 2800 Ma, 2600 Ma and 1730–1760 Ma on zircons from the Pointe Géologie Archipelago. Peucat et al. (2002) measured U–Pb ages of ~1600 Ma on zircons from clasts collected out of moraines exposed in Adélie Land, which they interpreted to have been connected to the Gawler Range volcanics and Hiltuba Suite granites of the Gawler craton in Australia; the Gawler Range volcanics and Hiltuba Suite granites have U–Pb zircon ages of 1580–1600 Ma (Fanning et al., 1988; Creaser and Fanning, 1993; Fanning et al., 2007).

$^{40}Ar/^{39}Ar$ hornblende ages show peaks at ~1608 Ma and 1715 Ma, and $^{40}Ar/^{39}Ar$ biotite ages show a peak at ~1626 Ma. These ages are consistent with $^{40}Ar/^{39}Ar$ hornblende (~1700) and biotite outcrop ages from George V Land (Fig. 5a–c; Di Vincenzo et al. (2007)). An additional but small ~1480 Ma peak in the $^{40}Ar/^{39}Ar$ hornblende ages has previously been attributed to the Mertz shear zone area (Pierce et al., 2011), as these ages are from a core site (Core 22) directly off the coast from this feature. The shear zone is dated at ~1500 Ma via $^{40}Ar/^{39}Ar$ biotite ages (Di Vincenzo et al., 2007), and Pierce et al. (2011) concluded that because

the shear zone extends far inland (Ferraccioli et al., 2009), it is likely that interior rocks were affected by this event. This means that $^{40}Ar/^{39}Ar$ hornblende ages from the interior could have been reset, thus explaining the ~1480 peak in the $^{40}Ar/^{39}Ar$ hornblende ages.

6.1.4.1.2. Ross orogeny. Core 23, located at the western edge of Adélie Land is characterized by >1400 Ma $^{40}Ar/^{39}Ar$ hornblende ages, which is consistent with the proximal on-land geology, yet both the detrital zircon U–Pb and $^{40}Ar/^{39}Ar$ biotite populations contain a population of grains with Ross orogen ages in addition to the >1400 Ma population. Pierce et al. (2011) reported hornblende and biotite $^{40}Ar/^{39}Ar$ ages from this core, and attributed the ~500 Ma biotite population to possible low-temperature re-setting in western Adélie Land. The presence of Ross-aged detrital zircons implies that this population is the result of ice-rafting from east of the Mertz shear zone, or alternatively that bedrock affected by the Ross orogen is more extensive than previously thought. We consider the latter explanation highly unlikely, given the distance between Core 23 and outcrops affected by the Ross orogen, as well as the absence of known Ross overprinting west of the Mertz shear zone.

6.1.4.1.3. Bowers terrane. Detrital zircon U–Pb and $^{40}Ar/^{39}Ar$ biotite ages show populations of ~389 Ma and ~369 Ma, respectively; this age population is notably absent from the hornblende grains. These ages most likely reflect sourcing from the Bowers Range, which has K–Ar dates of this age (Adams, 2006). The absence of hornblende grains in this age range is likely a lithological bias, in that source rocks do not contain appreciable amounts of hornblende.

6.1.4.1.4. McMurdo volcanics. $^{40}Ar/^{39}Ar$ hornblende grains from cores off the coast of NVL contain a population of young grains, with a peak age of 2.3 Ma; these ages were not found in either the detrital zircon U–Pb or $^{40}Ar/^{39}Ar$ biotite age populations. A likely source for these young grains is the McMurdo Group volcanic rocks found off the coast of Victoria Land in the western (East Antarctic side) Ross Sea. Armstrong (1978) measured K–Ar ages on 91 samples of volcanic rocks from the Transantarctic Mountains and Ross Sea islands, finding that the majority of the samples are 0.003 to 4.0 Ma, with only a few between 13.0 and 18.0 Ma. Cooper et al. (2007) dated volcanism associated with White Island at ~5–7 Ma, while Rilling et al. (2007) dated volcanism associated with the Terror Rift at <~4 Ma (see Kyle (2013) for a review of the McMurdo Volcanic Group).

6.1.4.2. Novel and previously un-described age populations

6.1.4.2.1. Grenvillian ages. There is a small spread of 1000–1200 Ma Grenvillian ages in the Adélie/George V/northern Victoria Land sector samples; there are small peaks of ~1057 and 1235 Ma in the U–Pb zircon data, though no apparent peaks in the $^{40}Ar/^{39}Ar$ hornblende or biotite data. While no Grenvillian ages have been reported from outcrops in the AL/GVL/NVL sector, Goodge and Fanning (2010) also found a small number of Grenvillian detrital U–Pb zircon ages from marine sediment samples in this area, consistent with our finding. Goodge and Fanning (2010) proposed that the presence of these ages are the result of either Grenvillian-aged basement extending to this part of the craton under the ice sheet, or the result of zircon recycling into sedimentary rocks present in the area. Given the presence of Grenvillian $^{40}Ar/^{39}Ar$ hornblende and biotite ages, however, it is more likely that there is in fact Grenvillian-aged basement under the ice sheet in this part of Antarctica, as hornblende and biotite grains would not have survived multiple sedimentary cycles.

6.1.4.2.2. Precursor to Ross orogeny?. Detrital zircon U–Pb ages from Adélie/GeorgeV/northern Victoria Land show two peaks, ~579 Ma and ~502 Ma. While the younger ~502 Ma age peak is consistent with typical Ross orogen ages in this area of 490–544 Ma (e.g., Veevers (2012)), the ~579 Ma peak is significantly older. Goodge and Fanning (2010), found an older age population of ~580 Ma in cores east of the Mertz shear zone, consistent with our findings. These authors attribute the older ages to the likelihood that Ross orogeny magmatism began earlier than that recorded in the limited outcrops in the area. Several other studies also find evidence for Ross magmatism as early as 580–590 Ma (Goodge et al., 2004, 2010, 2012), indicating that this is an orogeny-wide phenomenon. $^{40}Ar/^{39}Ar$ hornblende and biotite ages have a single peak at ~493 Ma and ~494 Ma, respectively; these ages are consistent with Ross orogen ages found in on-land sites to the east of the Mertz shear zone (Fig. 5a–c; (Adams, 2006; Di Vincenzo et al., 2007; Goodge, 2007)).

6.2. Comparison of thermochronometers by sector

In this section we summarize some of the broad observations that can be made about thermochronology and potential provenance signals based on each of the individual mineral systems (Fig. 6).

First, in each of the sectors the data overall show the logical sequence of progressively younger ages when comparing the detrital U–Pb zircon to $^{40}Ar/^{39}Ar$ hornblende to $^{40}Ar/^{39}Ar$ biotite ages, respectively, as would be expected based upon the relative closure temperatures of each system (e.g., Fig. 3a).

Second, Pan-African, Ross and Grenvillian ages are pervasive around East Antarctica. However, the peak ages of these events are variable, depending upon the area analyzed and the chronometer used, allowing for the potential to still differentiate between broad areas affected by these events. For example, while Grenvillian ages in each of the mineral systems are generally consistent (allowing for cooling following the event, as discussed above), the oldest peak Grenvillian ages are found in Wilkes Land (~1200–1100 Ma), followed by Dronning Maud Land (~1100–1000 Ma), and Prydz Bay (~1000–900 Ma) (see also Fitzsimons (2000)). In contrast, $^{40}Ar/^{39}Ar$ hornblende and biotite ages of Pan-African and Ross overprinting around East Antarctica generally show more overlap between the different sectors, but peak ages within these populations still show subtle variations (e.g., slightly older ages in the Prydz Bay area as compared to the Dronning Maud and George V Land locations) that may be applied to differentiate source terranes.

Third, each individual geographic sector described here carries a unique thermochronological fingerprint. Our detrital U–Pb zircon, $^{40}Ar/^{39}Ar$ hornblende and $^{40}Ar/^{39}Ar$ biotite ages for the Dronning Maud Land area present the first onshore/offshore comparison of its kind and an attempt to characterize the provenance signal. Overall, Dronning Maud Land is characterized by Grenvillian ages (1000–1100 Ma) and Pan-African/Ross ages in each of the thermochronometers. Archean $^{40}Ar/^{39}Ar$ hornblende and biotite ages are associated with the Grunhogna craton (~2°W to 15°W), and stand out as unique provenance indicator in this sector (Fig. 6). The peak ages for each of the chronometers associated with both tectonometamorphic events generally shows a younging trend from U–Pb to $^{40}Ar/^{39}Ar$ hornblende to $^{40}Ar/^{39}Ar$ biotite, as is to be expected given the different closure temperatures. Additionally, there appears to be a division in the $^{40}Ar/^{39}Ar$ biotite ages, in which Coats Land (~20°W to 30°W) is dominated by Grenvillian $^{40}Ar/^{39}Ar$ biotite ages (reflecting the lack of Pan-African overprinting in this area (Jacobs and Thomas, 2004)), while areas to the east of Coats Land are mostly in the 400–600 Ma range, with the exception of the area around the Grunhogna craton.

The Prydz Bay sector shows complete resetting of lower temperature thermochronometers during the Pan-African orogeny, as shown by the lack of Grenvillian aged $^{40}Ar/^{39}Ar$ hornblende and biotite ages. On the other hand, the Wilkes Land sector is the only one of the four geographic sectors that is not characterized by Pan-African/Ross ages (i.e. in core sites proximal to the continent). U–Pb zircon ages offer a unique ~1562 Ma population to aid in provenance work, while all chronometers have peak ages in the 1100–1200 Ma range, easily distinguishable from Grenvillian ages in different sectors (Fig. 6).

The sector is the most diverse. This sector is dominated by Ross ages (480–590 Ma), but also reveals significant proportions of grains with ages >1400 Ma (restricted to Adélie Land), and younger ages (389 and 369 Ma peak ages in the detrital zircon U–Pb and $^{40}Ar/^{39}Ar$ biotite data, respectively), and 2.3 Ma in the $^{40}Ar/^{39}Ar$ hornblende ages from

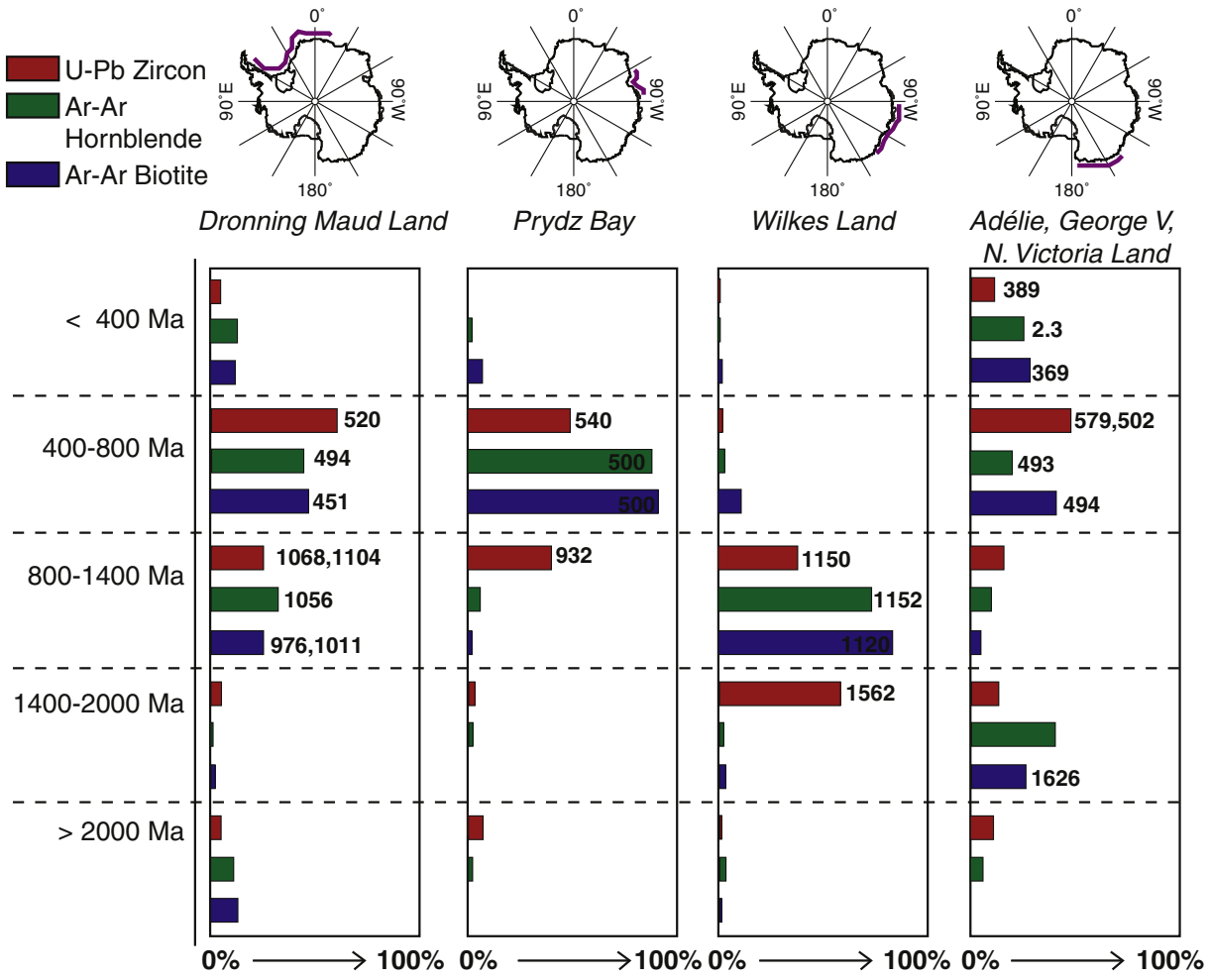

Fig. 6. Summary figure of U–Pb zircon (red), $^{40}Ar/^{39}Ar$ hornblende (green) and $^{40}Ar/^{39}Ar$ biotite (blue) ages. Thick pink line around map of Antarctica shows geographic coverage of each sector (Dronning Maud Land, Prydz Bay, Wilkes Land, Adélie/George V/northern Victoria Land). Vertical axis shows age bins, horizontal axis shows the percentage of ages, across the entire population of a given mineral in that sector, that fall within the corresponding age bin. (For the color version of this figure, the reader is referred to the web version of this article.)

cores located off of the George V/northern Victoria Land. U–Pb zircon ages in this sector contain a hint that the Ross orogeny in East Antarctica may extend as far back as 579 Ma.

Fourth, the potential power in using U–Pb zircon ages in addition to the $^{40}Ar/^{39}Ar$ thermochronometers is that it adds another level of characterization. Given the resilient nature of the U–Pb system in zircon, and zircon itself, additional age populations, not present in the $^{40}Ar/^{39}Ar$ hornblende and biotite ages of the source areas, are present, and can then be paired with these lower-temperature ages to better constrain potential source areas. Overall, the U–Pb zircon and $^{40}Ar/^{39}Ar$ hornblende and biotite ages that we have measured and discussed in this study faithfully reflect known neighboring on-land ages, and combined they offer ways to identify source areas of East Antarctica. An additional benefit of the detrital zircons is the potential for triple or double dating with fission track and/or (U–Th)/He (e.g., Cox et al., 2010; Tochilin et al., 2012; Thomson et al., 2013).

6.3. Ice-rafted zircons from ODP Site 1165

IRD provenance data can be interpreted to reflect changes in the Antarctic ice sheet through time, if ice and iceberg transport in the past differed from the present day. For example, Williams et al. (2010) studied the IRD from five sediment layers at ODP Site 1165 for $^{40}Ar/^{39}Ar$ ages of ice-rafted hornblendes. They provided evidence for massive iceberg armadas originating from Adélie Land and Wilkes Land during the Pliocene. Subsequent work by Pierce et al. (2011) showed the viability of $^{40}Ar/^{39}Ar$ biotite ages as a tracer of IRD from the same layers in ODP Site 1165.

Here we test the application of U–Pb zircon ages for determining the provenance of IRD. To our knowledge, this is the first study that attempts to use U–Pb zircon ages for this purpose in the Southern Ocean. We hence conducted our pilot study on exactly the same five samples from ODP Site 1165 analyzed by Williams et al. (2010) and Pierce et al. (2011), the depositional ages of which span ~19 to 3 Ma. Based on Williams et al. (2010) and Pierce et al. (2011), each of the five IRD layers contains a local, Prydz Bay provenance signature (~500 Ma) (Fig. 4). While the ~500 Ma age dominates the 19 Ma old IRD layer, the IRD samples deposited 7.0 and 3.0 Ma also contain grains with a Wilkes Land signature (~1100–1220 Ma) (Fig. 4), indicating sourcing of massive iceberg armadas from the Wilkes Land region to ODP Site 1165, a minimum distance of 1000 km to the east. The $^{40}Ar/^{39}Ar$ ages of hornblendes from the IRD layer from 4.65 Ma (100 cm) contains an additional age population of 1500–1600 Ma, reflecting potential sourcing from the Adélie Land margin, approximately 3000 km to the east.

6.3.1. Comparison of zircon, hornblende and biotite provenance (ODP Site 1165)

Zircons are relatively rare in Site 1165 sediments (n = 3 to 31 with an average of 15; Figs. 4 and 5A) compared to hornblende (n = 23 to 41

with an average of 33; Figs. 4 and 5B) and biotite grains (n = 28 to 41 with an average of 36; Figs. 4 and 5C), and all zircons that were found were analyzed. Despite the small number of analyses some interesting insights to the application of U–Pb zircons as a provenance tool for IRD are revealed by comparing the provenance of IRD deposited at ODP Site 1165 as determined by U–Pb zircon, $^{40}Ar/^{39}Ar$ hornblende and $^{40}Ar/^{39}Ar$ biotite.

6.3.1.1. Local Prydz Bay signature. Based on the characterization of source areas through our detrital U–Pb data from the shelf diamict and core-top IRD samples, and onshore data, we would expect the local Prydz Bay signature for the U–Pb zircons to include a 500–600 Ma population, potentially a small ~700 Ma population, and a Grenvillian population dominated by 900–1000 Ma ages (Figs. 3B and 5A; see also (Roy et al., 2007b; van de Flierdt et al., 2008; Tochilin et al., 2012)).

Each of the depositional layers (where populations exist) have in common grains in the 400–600 Ma range (Fig. 4), consistent with IRD sourced from the local Prydz Bay region, with U–Pb zircon ages slightly older than $^{40}Ar/^{39}Ar$ hornblende ages, which are slightly older than $^{40}Ar/^{39}Ar$ biotite, as would be expected by the low closure temperatures of $^{40}Ar/^{39}Ar$ hornblende (~500 °C) and $^{40}Ar/^{39}Ar$ biotite (~300 °C) systems in comparison to U–Pb zircon (>900 °C). This is in agreement with what is observed in the proximal sediment core samples discussed in Section 6.2, and previous work (Roy et al., 2007b; van de Flierdt et al., 2008; Tochilin et al., 2012). Overall, the inferred source based on each of the provenance tools is consistent with regards to a local Prydz Bay source.

What is surprising, though, is that we do not observe a population of zircons with a U–Pb ages between 900 and 1000 Ma in any of the samples, which is the second-most dominant age population for this sector, based on both onshore studies and the detrital samples from this and previous work (Fig. 5a).

6.3.1.2. Wilkes Land signature. Layers deposited at 3.0 Ma and 7.0 Ma show a second population of grains with ages 1100–1300 Ma, reflecting, for each chronometer, a Wilkes Land provenance. As seen with the 400–600 Ma populations, there is a progressive younging of the peaks from U–Pb zircon to $^{40}Ar/^{39}Ar$ hornblende to $^{40}Ar/^{39}Ar$ biotite ages. This Wilkes Land signature should also contain detrital U–Pb zircon age populations of ~1560 Ma due to the abundance of these ages in IRD offshore Wilkes Land (Figs. 3C and 5a), and yet this population is absent. In both samples, it may be that our proximal core sites used for comparison with onshore data are tapping a larger area than the ice streams that produced the iceberg armadas inferred in the late Miocene and Pliocene by Williams et al. (2010).

6.3.1.3. Potential Adélie Land signature?. The only IRD layer in which the different approaches appear to provide contradictory provenance information is the 4.65 Ma layer sampled in ODP Site 1165, Core 6H, Section 1 at 100–102 cm depth (Fig. 4, third sample from the top; note this is different from the 4.65 Ma depositional layer sampled in ODP Site 1165, Core 6H, Section 1 at 70–72 cm depth plotted above). Both U–Pb and $^{40}Ar/^{39}Ar$ hornblende data contain the expected local 400–600 Ma population, but the detrital zircon U–Pb ages show a second population of 1100–1200 Ma, while the $^{40}Ar/^{39}Ar$ hornblende ages show a second population of 1500–1600 Ma. In comparing the zircon and hornblende age populations from the 4.65 Ma (100 cm) layer, we see that 10% and 34% of the hornblende grains fall in the 1000–1200 Ma and 1400–1600 Ma rage, respectively (n total is 41). Conversely, 52% and 4% of the zircon ages fall in the 1000–1200 Ma and 1400–1600 Ma populations (n total is 21). The source characterization based upon U–Pb zircon ages would imply that the 1100–1200 Ma zircon population is sourced from Wilkes Land, while the source characterization based upon the $^{40}Ar/^{39}Ar$ hornblende ages, as shown by Williams et al. (2010), was interpreted as sourcing from Adélie Land. One possible explanation for this discrepancy is the potential for a lithologic bias in material eroded by ice streams along the Wilkes and Adélie Land margins that was subsequently deposited at ODP Site 1165. For example, it could be that zircon-rich, hornblende-poor material was sourced from Wilkes Land, while hornblende-rich, zircon-poor material was sourced from Adélie Land. A second explanation is that the zircons are in fact sourced from Adélie Land, and in agreement with the $^{40}Ar/^{39}Ar$ hornblende data. While Adélie Land and George V Land west of the Mertz shear zone contain a dominant $^{40}Ar/^{39}Ar$ hornblende age population of 1400–1700 Ma (Cores 23–25), the U–Pb zircon ages from this area have small population of 1000–1200 Ma (~10%) and an even smaller 1400–1600 Ma (4%) population. Thus, zircons sourced from this area would not be expected to contain abundant grains in the 1400–1600 Ma population relative to the 1000–1200 Ma population. This particular sample highlights the importance of using multiple provenance tracers.

7. Other multichronometer approaches

In this study we have discussed applying the combination of detrital U–Pb zircon, $^{40}Ar/^{39}Ar$ hornblende and $^{40}Ar/^{39}Ar$ biotite ages in order to 1) constrain more fully East Antarctica's subglacial geology, and 2) apply this information to determine the provenance of ice-rafted zircon grains deposited at ODP Site 1165 in the Neogene. This work highlights the value in applying multiple chronometers to better understand East Antarctica's obscured geology as well as its ice sheet history. Here we provide a brief overview of other studies that use multiple chronometers within and across multiple minerals to constrain East Antarctica's subglacial geology, in the hope these approaches will continue to be used to examine broad questions about East Antarctica's geology, landscape evolution and ice sheet history. As discussed in Section 2, the advantage to multiple chronometers is that different chronometers retain their ages at different temperatures (U–Pb in zircon (crystallization age), $^{40}Ar/^{39}Ar$ in hornblende (~500 °C), U–Pb in apatite (~500 °C), $^{40}Ar/^{39}Ar$ in muscovite (~400 °C) $^{40}Ar/^{39}Ar$ in biotite (~350 °C), fission track in zircon (~250 °C), (U–Th)/He in zircon (~180 °C), fission track in apatite (~100 °C), (U–Th)/He in apatite (~70 °C) (Reiners et al., 2005b)). By combining one or more, a more complete interpretation of the geological and erosion history of an area can be obtained.

Addressing the origin of the subglacial Gamburtsev Mountains in East Antarctica, van de Flierdt et al. (2008) examined Eocene fluvial-deltaic sediments recovered from ODP Site 1166 (Prydz Bay). Based upon pre-glacial drainage reconstructions, van de Flierdt et al. (2008) argued that there would have been significant erosion and sediment delivery to this core site via transportation by rivers from the Gamburtsev Mountains through the Lambert Graben. van de Flierdt et al. (2008) measured detrital $^{40}Ar/^{39}Ar$ hornblende, biotite and muscovite ages along with U–Pb zircon ages, and all chronometers showed distinct ~500 Ma populations. Paired with analyses of neodymium isotopes in bulk sediments, these authors concluded that there was no evidence for recent volcanic activity, and hence rejected the hypothesis that the Gamburtsev Mountains have a young, volcanic origin.

Palmer et al. (2012) also took a multichronometer approach, measuring detrital U–Pb zircon and $^{40}Ar/^{39}Ar$ hornblende and mica ages from tills collected from the Byrd Glacier area of the Transantarctic Mountains, where the locally exposed bedrock consists of the Beacon Supergroup. The goal of this study was to use tills (dispersed grains and clasts) sourced from within the East Antarctic craton to further constrain the subglacial geology of a portion of East Antarctica. Detrital U–Pb zircon ages were measured from the coarse sand fraction of the till, while $^{40}Ar/^{39}Ar$ hornblende and mica ages were measured on both detrital grains and grains from individual till clasts. Each of the chronometers showed Pan-African and/or Ross age populations, with the detrital U–Pb zircon ages containing additional Grenvillian (950–1270 Ma) and Late Archean (~2700 Ma) populations, and the $^{40}Ar/^{39}Ar$ hornblende ages a Grenvillian (1150–150 Ma) population. Palmer et al. (2012) highlight two key aspects of this approach, in that 1) the presence of detrital hornblende and micas indicates sourcing from primary bedrock, as these

minerals are unlikely to be sourced from the local Beacon Supergroup strata, and 2) that by pairing geochronological measurements from dispersed grains with those from clasts, an evaluation may be made of how representative ages from a single clast are.

Studies based upon detrital zircons and apatites have the additional benefit of the potential for triple or double dating individual grains with a combination of U–Pb, fission track and/or (U–Th)/He ages, e.g., (Reiners et al., 2005a). Through the double or triple dating of these grains, individual thermal, and thus uplift and erosional histories of the source rocks, can be determined, as well as provenance. Cox et al. (2010), also investigating the subglacial Gamburtsev Mountains, double dated detrital apatite grains (recovered from Eocene fluvial-deltatic sediments at ODP Site 1166 in Prydz Bay) using (U–Th)/He and apatite fission track dating, and concluded that grains sourced from the Gamburtsevs experienced extremely low erosion rates (0.01 to 0.02 km/Myr for at least the past 250 Myr). Tochilin et al. (2012) applied $^{40}Ar/^{39}Ar$ hornblende ages, triple dating of apatites (U–Pb, fission track and (U–Th)/He) and double dating of zircons (U–Pb and fission track) to detrital grains from Oligocene to Quaternary aged glacial diamicts recovered at ODP Site 739 (Prydz Bay), to look at long term tectonic and erosion history in the Lambert Graben region of East Antarctica. Using this combination of methods they were able to infer relatively higher erosion rates in the Oligocene, after the initiation of widespread East Antarctic glaciation, followed by slower rates from the late Miocene onwards. Thomson et al. (2013) triple dated apatite using U–Pb, fission track and (U–Th)/He ages and measured zircon fission track ages in detrital sediments (glacial moraines and offshore glacial sediments) in the Lambert Graben/Prydz Bay area in order to look at long-term (late Cretaceous through Quaternary) erosion rates and constrain subglacial landscape evolution. These authors found that the local overdeepened fjord topography beneath the Lambert Glacier, inferred by aerogeophysical surveys, was created in the past 34 Ma, after major ice sheet expansion on East Antarctica.

While each of the aforementioned studies was based upon single or multi-dating of individual grains, a clear objective for future work would be to apply the same approach(es) to grains within individual cobbles or clasts. Just as double and triple dating of apatites and zircons allows for reconstructing that grain's individual history, multiple chronometers across different minerals would allow for even more age measurements that are guaranteed to have been sourced from the same area and have the same history, as the grains are all from the same clast. This approach would be especially useful for provenance studies, as we could identify multiple ages within a single clast for both a more specific source area identification and for better elucidating the source region's thermal time-temperature history.

8. Conclusions

In this paper we have performed a comparison of detrital U–Pb zircon, $^{40}Ar/^{39}Ar$ hornblende, and $^{40}Ar/^{39}Ar$ biotite ages from 27 marine sediment cores, adding a total of 3284 new analyses to a growing data set of detrital thermochronologic ages from glacial-marine sediments around East Antarctica. Included in this is the first analysis of ice-rafted U–Pb zircon ages from a down-core record of IRD in ODP Site 1165 located offshore Prydz Bay. Our results lead us to reach the following conclusions:

(1) Detrital U–Pb zircon, $^{40}Ar/^{39}Ar$ hornblende and $^{40}Ar/^{39}Ar$ biotite ages match well with the ages of outcrops nearby on Antarctica, indicating that detrital ages can also faithfully represent the ages of ice-covered areas. Major populations present in our samples include Archean ages reflecting the Grunehogna and Terre Adélie cratons, Paleoproterozoic ages (~1500–1700 Ma) reflecting thermal events in Wilkes and Adélie Land, Grenvillian (1330–900 Ma), Pan-African (600–450 Ma) and Ross (590–480 Ma) ages reflecting three major orogenies in East Antarctica's history, an ~380 Ma population reflecting volcanic activity in the Bowers Terrane of northern Victoria Land, a ~180 Ma population of grains reflecting Ferrar–Karoo magmatism associated with Jurassic rifting and separation of Gondwanaland, and a 0–20 Ma population reflecting the McMurdo volcanics in the Ross Sea.

(2) Our results reveal age populations from the detrital U–Pb zircon, $^{40}Ar/^{39}Ar$ hornblende and $^{40}Ar/^{39}Ar$ biotite measurements which have not been reported from on-shore studies, reflecting the presence of ice-covered terranes that are not accessible for direct study, or were unsampled (U–Pb zircon ages dominate the on-land record). The previously unrecorded age populations found in this study (Archean $^{40}Ar/^{39}Ar$ hornblende and biotite ages in Dronning Maud Land; early (?) Grenvillian $^{40}Ar/^{39}Ar$ hornblende ages (1200–1300) in the Weddell Sea; ~1560 Ma population of U–Pb zircons from the Wilkes Land margin; Grenvillian (1000–1200 Ma) U–Pb zircon ages from the Adélie/George V Land margin; and an older, potentially Ross orogen related population of ~580 Ma from the Adélie/George V Land margin) illustrate both the importance and potential for future studies of this kind as a means of learning more about East Antarctica's geology.

(3) Zircon, hornblende and biotite grains were found in variable amounts, as expected, in each of the core samples, reflecting differences in the lithologies of the bedrock eroded by the ice sheet. U–Pb zircon, $^{40}Ar/^{39}Ar$ hornblende and $^{40}Ar/^{39}Ar$ biotite age populations were found to not always be consistent between each of the individual samples. In some cases, this can be attributed to lithological bias, while in many it is more likely the result of resetting of the $^{40}Ar/^{39}Ar$ hornblende and $^{40}Ar/^{39}Ar$ biotite systems.

(4) As has been shown in the previous works (Roy et al., 2007b; Williams et al., 2010; Pierce et al., 2011), East Antarctica can be broadly divided by the lower-temperature chronometers into source areas with distinctive ages: northern Victoria Land west to the Mertz Glacier in George V Land, Adélie Land, Wilkes Land, and Prydz Bay each have a unique signature. Dronning Maud Land as a whole is a mix of Grenvillian and Pan-African/Ross-orogen ages, however within this sector divisions can be made to determine source areas.

(5) U–Pb zircon measurements made on ice-rafted deposits from ODP Site 1165 highlight both the potential and disadvantage for using this approach to trace the provenance of IRD from deep-sea core sites, with the disadvantage being low abundance of zircons in each of the IRD layers

(6) The results of this comparative approach are promising, and we recommend that further application of this combined approach is likely to improve our understanding of East Antarctic geology, particularly in areas that are ice-covered. While the cores in this study were chosen so as to characterize major crustal elements of East Antarctica, more detailed work in specific study areas (e.g., Wilkes Land margin, which only has a few outcrops), combined with other types of zircon analyses, e.g., zircon grain morphology, fission track and (U–Th)/He, and/or other mineral grain thermochronometers, will undoubtedly prove more insights to East Antarctica's geologic history.

Supplementary data to this article can be found online at http://dx.doi.org/10.1016/j.earscirev.2014.08.010.

Acknowledgments

Research was partially supported by NSF grant ANT-0538580 to Hemming, Goldstein and van de Flierdt, ANT 09-44489 to Williams, Hemming and van de Flierdt, ANT 08-38722 and ANT 08-38729 to Reiners, Thomson and Gehrels (U of AZ) and Hemming (LDEO) and NSF grant EAR 10-32156 which provided support to the Arizona Laserchron center. We thank E. Dahlhauser, E. Steponaitis, S. Cox, G.

Mesko, E. Palmer and M. Reitz for the assistance in sample processing at LDEO; G. Ali, D. Giesler, M. Pecha and the AZ Laserchron center for the assistance with zircon analyses; and the FSU Antarctic Marine Geology Research Facility and the Integrated Ocean Drilling Program for core samples. Special thanks to the 'ANTARCTICHRON' workshop (University of Arizona in June 2011), during which many of the U–Pb zircon analyses were made. The authors would like to thank John Goodge and Joachim Jacobs for careful and constructive reviews.

References

Aalto, K.R., Sharp, W.D., Renne, P.R., 1998. $^{40}Ar/^{39}Ar$ dating of detrital micas from Oligocene–Pleistocene sandstones of the Olympic Peninsula, Klamath Mountains, and northern California Coast Ranges: provenance and palaeodrainage patterns. Can. J. Earth Sci. 35, 735–745.

Adams, C.J., 2006. Style of uplift of Paleozoic Terranes in Northern Victoria Land, Antarctica: evidence from K–Ar age patterns. In: Futterer, D.K., Damaske, D., Kleinschmidt, G., Miller, H., Tessensohn, F. (Eds.), Antarctica: Contributions to global earth sciences. Springer-Verlag, Berlin Heidelberg, New York, NY, pp. 205–214.

Andersen, T., 2005. Detrital zircons as tracers of sedimentary provenance: limiting conditions from statistics and numerical simulation. Chem. Geol. 216, 249–270.

Anderson, J.B., 1999. Antarctic Marine Geology, Cambridge.

Armstrong, R.L., 1978. K–Ar dating: Late Cenozoic McMurdo Volcanic Group and dry valley glacial history, Victoria Land, Antarctica. N. Z. J. Geol. Geophys. 21, 685–698.

Arndt, N.T., Todt, W., Chauvel, C., Tapfer, M., Weber, K., 1991. U–Pb zircon age and Nd isotopic composition of granitoids, charnockites and supracrustal rocks from Heimefrontfjella, Antarctica. Geol. Rundsch. 80, 759–777.

Avigad, D., Stern, R.J., Beyth, M., Miller, N., McWilliams, M.O., 2007. Detrital zircon U–Pb geochronology of Cryogenian diamictites and Lower Paleozoic sandstone in Ethiopia (Tigrai): age constraints on Neoproterozoic glaciation and crustal evolution of the southern Arabian–Nubian Shield. Precambrian Res. 154, 88–106.

Barton, J.M., Klemd, R., Allsopp, H.L., Auret, S.H., Copperthwaite, Y.E., 1987. The geology and geochronology of the Annandagstoppane granite, Western Dronning Maud Land, Antarctica. Contrib. Mineral. Petrol. 97, 488–496.

Bateman, R.M., Catt, J.A., 1985. Modification of heavy mineral assemblages in English coversands by acid pedochemical weathering. Catena 12, 1–21.

Bickford, M.E., Chase, R.B., Nelson, B.K., Shuster, R.D., Arruda, E.C., 1981. U–Pb studies of zircon cores and overgrothws, and monazite: implications for age and petrogenesis of the northeastern Idaho batholith. J. Geol. 89, 433–457.

Bisnath, A., Frimmel, H.E., Armstrong, R.A., Board, W.S., 2006. Tectono-thermal evolution of the Maud Belt: New SHRIMP U–Pb zircon data from Gjelsvikfjella, Dronning Maud Land, East Antarctica. Precambrian Res. 150, 95–121.

Black, L.P., Sheraton, J.W., 1990. The influence of Precambrian source components on the U–Pb zircon age of a Palaeozoic granite from northern Victoria Land, Antarctica. Precambrian Res. 46, 275–293.

Black, L.P., Sheraton, J.W., Tingey, R.J., McCulloch, M.T., 1992. New U–Pb zircon ages from the Denman Glacier area, East Antarctica, and their significance for Gondwana reconstruction. Antarct. Sci. 4, 447–460.

Board, W.S., Frimmel, H.E., Armstrong, R.A., 2005. Pan-African tectonism in the Western Maud Belt: P–T–t path for high-grade gneisses in H.U. Sverdrupfjella, East Antarctica. J. Petrol. 46, 671–699.

Boger, S.D., 2011. Antarctica — before and after Gondwana. Gondwana Res. 19, 335–371.

Boger, S.D., Carson, C.J., Wilson, C.L.J., Fanning, C.M., 2000. Neoproterozoic deformation in the Radok Lake region of the northern Prince Charles Mountains, East Antarctica; evidence for a single protracted orogenic event. Precambrian Res. 104, 1–24.

Boswell, P.G.H., 1923. Some aspects of the petrology of sedimentary rocks. Proc. Liverpool Geol. Soc. 13, 231–303.

Bowen, N.L., 1922. The reaction principle in petrogenesis. J. Geol. 30, 178–198.

Carson, C.J., Boger, S.D., Fanning, C.M., C.J.L., W., Thost, D.E., 2000. SHRIMP U–Pb geochronology from Mount Kirby, northern Prince Charles Mountains, East Antarctica. Antarct. Sci. 12, 429–442.

Clarkson, P.D., Brook, M., 1977. Age and position of the Ellsworth Mountains crustal fragment, Antarctica. Nature 265, 615–616.

Cohen, H.A., Hall, C.M., Lundberg, N., 1995. $^{40}Ar/^{39}Ar$ dating of detrital grains constrains the provenance and stratigraphy of the Gravina belt, Southeastern Alaska. J. Geol. 103, 327–337.

Collins, A.S., Pisarevsky, S.A., 2005. Amalgamating eastern Gondwana: the evolution of the Circum-India Orogens. Earth-Sci. Rev. 71, 229–270.

Cooper, A.F., Adam, L.J., Coulter, R.F., Eby, G.N., McIntosh, W.C., 2007. Geology, geochronology and geochemistry of a basanitic volcano, White Island, Ross Sea, Antarctica. J. Volcanol. Geotherm. Res. 165, 182–216.

Cordani, U.G., D'Agrella-Filho, M.S., Brito-Neves, B.B., Trindade, I.F., 2003. Tearing up Rodinia: the Neoproterozoic paleogeography of South American cratonic fragments. Terra Nova 15, 350–359.

Cox, S.E., Thomson, S.N., Reiners, P.W., Hemming, S.R., van de Fleirdt, T., 2010. Extremely low long-term erosion rates around the Gamburtsev Mountains in interior East Antarctica. Geophys. Res. Lett. 37, 5.

Creaser, R.A., Fanning, C.M., 1993. A U–Pb zircon study of the Mesoproterozoic Charleston Granite, Gawler craton, South Australia. Aust. J. Earth Sci. 40, 519.

Curtis, M.L., Millar, I.L., Storey, B.C., Fanning, C.M., 2004. Structural and geochronological constraints of early Ross orogenic deformation in the Pensacola Mountains, Antarctica. Geol. Soc. Am. Bull. 116, 619–636.

Dalrymple, G.B., Alexander Jr., E.C., Lanphere, M.A., Kraker, G.P., 1981. Irradiation of samples for 40Ar/39Ar dating using the Geological Survey TRIGA reactor. Geological Society Professional Paper 1176.

Deer, W.A., Howie, R.A., Zussman, J., 1992. An Introduction to Rock-forming Minerals, 2nd edition. Longman Scientific and Technical, Essex, England.

Di Vincenzo, G.D., Talarico, F., Kleinschmidt, G., 2007. An $^{40}Ar/^{39}Ar$ investigation of the Mertz Glacier area (George V Land, Antarctica): implications for the Ross Orogen-East Antarctic Craton relationship and Gondwana reconstructions. Precambrian Res. 152, 93–118.

Downing, G.E., Hemming, S.R., Jost, A., Roy, M., 2013. $^{40}Ar/^{39}Ar$ hornblende provenance clues about Heinrich event 3 (H3), advances in $^{40}Ar/^{39}Ar$ dating: from archaeology to planetary sciences. Geological Society of London, Special Papers.

Duclaux, G., Rolland, Y., Ruffet, G., Ménot, R.-P., Guillot, S., Peucat, J.-J., Fanning, M., Rey, P., Pêcher, A., 2008. Superimposed Neoarchaean and Paleoproterozoic tectonics in the Terre Adélie Craton (East Antarctica): evidence from Th–U–Pb ages on monazite and $^{40}Ar/^{39}A$ ages. Precambrian Res. 167, 316–338.

Duncan, R.A., Hooper, P.R., Rehacek, J., Marsh, J.S., Duncan, A.R., 1997. The timing and duration of the Karoo igneous event, southern Gondwana. J. Geophys. Res. 101, 18127–18138.

Fanning, C.M., Flint, R.B., Parker, A.J., Ludwig, K.R., Blissett, A.H., 1988. Refined Proterozoic evolution of the Gawler craton, South Australia, through U–Pb zircon geochronology. Precambrian Res. 40 (41), 363–386.

Fanning, C.M., Reid, A.J., Teale, G.S., 2007. A geochronological framework for the Gawler Craton, South Australia. South Australia. Geological Survey Bulletin. 55.

Fedo, C.M., Sircombe, K.N., Rainbird, R.H., 2003. Detrital zircon analysis of the sedimentary record. In: Hanchar, J.M., Hoskin, P.W.O. (Eds.), Rev. Mineral. Geochem. 277–303.

Ferraccioli, F., Armadillo, E., Jordan, T., Bozzo, E., Corr, H., 2009. Aeromagnetic exploration over the East Antarctic Ice Sheet: a new view of the Wilkes Subglacial Basin. Tectonophysics 478, 62–77.

Fitzsimons, I.C.W., 2000. Grenville-age basement provinces in East Antarctica: evidence for three separate collisional origins. Geology 28, 879–882.

Fitzsimons, I.C.W., 2003. Proterozoic basement provinces of southern and southwestern Australia, and their correlation with Antarctica. Geol. Soc. Lond. Spec. Publ. 206, 93–130.

Fitzsimons, I.C.W., Kinny, P.D., Harley, S.L., 1997. Two stages of zircon and monazite growth in anatectic leucogneiss: SHRIMP constraints on the duration and intensity of Pan-African metamorphism in Prydz Bay, East Antarctica. Terra Nova 9, 47–51.

Flemming, T.H., Foland, K.A., Elliot, D.H., 1995. Isotopic and chemical constraints on the crustal evolution and source signature of Ferrar magmas, north Victoria Land, Antarctica. Contrib. Mineral. Petrol. 121, 217–236.

Flowerdew, M.J., Tyrrell, S., Riley, T.R., Whitehouse, M.J., Mulvaney, R., Leat, P.T., Marschall, H.R., 2012. Distinguishing East and West Antarctic sediment sources using the Pb isotope composition of detrital K-feldspar. Chem. Geol. 292–293.

Furnes, H., Mitchell, J.G., 1978. Age relationships of Mesozoic basalt lava and dykes in Vestfjella Dronning Maud Land, Antarctica. Nor. Polarinst. Skr. 169, 45–68.

Furnes, H., Vad, E., Austrheium, H., Mitchell, J.G., Garmann, L.B., 1987. Geochemistry of basalt lavas from Vestt]ella and adjacent areas, Dronning Maud Land, Antarctica. Lithos 337–356.

Gaudette, H.E., Vitrac-Michard, A., Allègre, C.J., 1981. North American Precambrian history recorded in a single sample: high-resolution U–Pb systematics of the Potsdam Sandstone detrital zircons, New York State. Earth Planet. Sci. Lett. 52, 248–260.

Gehrels, G., 2012. Detrital zircon U–Pb geochronology: current methods and new opportunities. In: Busby, C., Azor, A. (Eds.), Tectonics of Sedimentary Basins: Recent AdvancesTectonics of Sedimentary Basins: Recent Advances. Wiley-Blackwell Publishing, pp. 47–62.

Gehrels, G., Valencia, V., Pullen, A., 2006. Detrital zircon geochronology by laser-ablation multicollector ICPMS at the Arizona LaserChron Center. In: Olszewski, T. (Ed.), Geochronology: Emerging Opportunities, Paleonotological Society Short Course, October 21, 2006, Philadelphia, PAPaleontological Scoicety Papers. vol. 12. The Paleontological Society.

Gehrels, G.E., Valencia, V.A., Ruiz, J., 2008. Enhanced precision, accuracy, efficiency, and spatial resolution of U–Pb ages by laser ablation-multicollector-inductively coupled plasma-mass spectrometry. Geochem. Geophys. Geosyst. 9.

Gehrels, G.E., Kapp, P., DeCelles, P., Pullen, A., Blakey, R., Weislogel, A., Ding, L., Guynn, J., Martin, A., McQuarrie, N., Yin, A., 2011a. Detrital zircon geochronology of pre-Tertiary strata in the Tibetan–Himalayan orogen. Tectonics 30.

Gehrels, G.E., Blakey, R., Karlstrom, K.E., Timmons, J.M., Dickinson, B., Pecha, M., 2011b. Detrital zircon U–Pb geochronology of Paleozoic strata in the Grand Canyon, Arizona. Lithosphere 3.

Goldich, S.S., 1938. A study in rock weathering. J. Geol. 46, 17–58.

Goodge, J.W., 2007. Metamorphism in the Ross orogen and its bearing on Gondwana margin tectonics. In: Cloos, M., Carlson, W.D., Gilbert, M.C., Liou, J.G., Sorensen, S.S. (Eds.), Convergent Margin Terranes and Associated Regions: A Tribute to W.G. Ernst, Geol. Soc. Amer. Special Paper, pp. 185–203.

Goodge, J.W., Fanning, C.M., 2010. Composition and age of the East Antarctic Shield in eastern Wilkes Land determined by proxy from Oligocene–Pleistocene glaciomarine sediment and beacon supergroup sandstones, Antarctica. Geol. Soc. Am. Bull. 122, 1135–1159.

Goodge, J.W., Myrow, P., Williams, I.S., Bowring, S., 2002. Age and provenance of the Beardmore Group, Antarctica: constraints on Rodininia supercontinent breakup. J. Geol. 110, 393–406.

Goodge, J.W., Williams, I.S., Myrow, P., 2004. Provenance of Neoproterozoic and lower Paleozoic siliciclastic rocks of the central Ross orogen, Antarctica: detrital record of rift-, passive- and active-margin sedimentation. Geol. Soc. Am. Bull. 116, 1253–1279.

Goodge, J.W., Fanning, C.M., Brecke, D.M., Licht, K.J., Palmer, E.F., 2010. Continuation of the Laurentian Grenville Province across the Ross Sea Margin of East Antarctica. J. Geol. 118, 601–619.
Goodge, J.W., Fanning, C.M., Norman, M.D., Bennett, V.C., 2012. Temporal, isotopic and spatial relations of Early Paleozoic Gondwana-margin arc magmatism, Central Transantarctic Mountains, Antarctica. J. Petrol. 1–39.
Gose, W.A., Helper, M.A., Connelly, J.N., Hutson, F.E., Dalziel, I.W.D., 1997. Paleomagnetic data and U–Pb isotopic age determinations from Coats Land, Antarctica: implications for late Proterozoic plate reconstructions. Geophys. Res. 101, 7889–7902.
Gwiazda, R.H., Hemming, S.R., Broecker, W.S., Onsttot, T., Mueller, C., 1996. Evidence from $^{40}Ar/^{39}Ar$ ages for a Churchill Province source of ice-rafted amphiboles in Heinrich layer 2. J. Glaciol. 42, 440–446.
Harley, S.L., Kelly, N.M., 2007. Ancient Antarctica: the Archaean of the East Antarctic shield. In: van Kranendonk, M.J., Smithies, R.H., Bennett, V.C. (Eds.), Developments in Precambrian Geology. Elsevier.
Harris, P.D., 1999. The geological evolution of Neumayerskarvet in the Northern Kirwanveggen, Western Dronning Maud Land, Antarctica. Rand Afrikaans University, Johannesburg, p. 249.
Harris, P.D., Moyes, A.B., Fanning, C.M., Armstrong, R.A., 1995. Zircon ion microprobe results from the Maudheim high-grade gneiss terrane, western Dronning Maud Land, Antarctica. In: Barton, J.M.J., Copperthwaite, Y.E. (Eds.), Centennial Geocongress. Geological Society of South Africa, Johannesburg, pp. 240–243.
Hemming, S.R., Hajdas, I., 2003. Ice-rafted detritus evidence from $^{40}Ar/^{39}Ar$ ages of individual hornblende grains for evolution of the eastern margin of the Laurentide ice sheet since 43 ^{14}C ky. Quat. Int. 99, 29–43.
Hemming, S.R., Broecker, W.S., Sharp, W.D., Bond, G.C., Gwiazda, J.F., 1998. Provenance of the Heinrich layers in core V28-82, northeastern Atlantic: $^{40}Ar–^{39}Ar$ ages of ice-rafted hornblende, Pb isotopes in feldspar grains, and Nd–Sr–Pb isotopes in the fine sediment fraction. Earth Planet. Sci. Lett. 164, 317–333.
Hemming, S.R., Bond, G.C., Broecker, W.S., Sharp, W.D., Klas-Mendelson, M., 2000. Evidence from $^{40}Ar/^{39}Ar$ ages of individual hornblende grains for varying laurentide sources of iceberg discharges 22,000 to 10,500 yr B.P. Quat. Res. 54, 372–373.
Hemming, S.R., Vorren, T.O., Kleman, J., 2002. Provinciality of ice rafting in the North Atlantic: application of $^{40}Ar/^{39}Ar$ dating of individual ice rafted hornblende grains. Quat. Int. 95–96, 75–85.
Hodges, K.V., Ruhl, K.W., Wobus, C.W., Pringle, M.S., 2005. $^{40}Ar/^{39}Ar$ thermochronology of detrital minerals. Rev. Mineral. Geochem. 58, 239–257.
Jackson, C., 1999. Characterization of Mesoproterozoic to Palaeozoic Crustal Evolution of Western Dronning Maud Land. Study 3: Deformational History and Thermochronology of the Central Kirwanveggen. Department of Environmental Affairs and Tourism, Pretoria, p. 80.
Jacobs, J., Thomas, R.J., 2004. Himalayan-type indenter-escape tectonics model for the southern part of the late Neoproterozoic–early Paleozoic East Africa-Antarctic orogen. Geology 32, 721–724.
Jacobs, J., Ahrendt, H., Kreutzer, H., Weber, K., 1995. K–Ar, $^{40}Ar–^{39}Ar$ and apatite fission-track evidence for Neoproterozoic and Mesozoic basement rejuvenation events in the Heimefrontfjella and Mannefallknausane (East Antarctica). Precambrian Res. 75, 251–262.
Jacobs, J., Bauer, W., Spaeth, G., Thomas, R.J., Weber, K., 1996. Lithology and structure of the Grenville-aged (1.1 Ga) basement of Heimefrontjella (East Antarctica). Geol. Rundsch. 85, 800–821.
Jacobs, J., Falter, M., Weber, K., Jebberger, E.K., 1997. Evidence for the structural evolution of the Heimefront Shear Zone (Western Dronning Maud Land), East Antarctica. In: Rico, C.A. (Ed.), The Antarctic Region: Geological Evolution and Processes. Terra Antarctica Publication, Siena, pp. 37–44.
Jacobs, J., Bauer, W., Fanning, C.M., 2003a. Late Neoproterozoic/Early Palaeozoic events in central Dronning Maud Land (East Antarctica) and significance for the southern extension of the EAO into East Antarctic. Precambrian Res. 126, 27–53.
Jacobs, J., Fanning, C.M., Bauer, W., 2003b. Timing of Grenville-age vs. Pan-African medium- to high grade metamorphism in western Dronning Maud Land (East Antarctica) and significance for correlations in Rodinia and Gondwana. Precambrian Res. 125, 1–20.
Jacobs, J., Klemd, R., Fanning, C.M., Bauer, W., Columbo, F., 2003c. Extensional collapse of the Late Neoproterozoic/Early Palaeozoic East African/Antarctic Orogen in central Dronning Maud Land. In: Yoshida, M., Windley, B.F., Dasgupta, S. (Eds.), Proterozoic East Gondwana: Supercontinent Assembly and Breakup. Geological Society, London.
Jacobs, J., Bingen, B., Thomas, R.J., Bauer, W., Wingate, M.T.D., Feitio, P., 2008. Early Palaeozoic orogenic collapse and voluminous late-tectonic magmatism in Dronning Maud Land and Mozamique: insights into the partially delaminated orogenic root of the East African-Antarctic Orogen? Geol. Soc. Lond., Spec. Publ. 308, 69–90.
Kinny, P.D., Black, L.P., Sheraton, J.W., 1993. Zircon ages and the distribution of Archaean and Proterozoic rocks in the Rauer Islands. Antarct. Sci. 5, 193–206.
Kleinschmidt, G., 2007. Geological evolution and structure of Antarctica. In: Riffenburgh, B. (Ed.), Encylopedia of the Antarctic. Routledge, New York/London, pp. 430–437.
Knutz, P.C., Storey, M., Kuihpers, A., 2013. Greenland iceberg emissions constrained by $^{40}Ar/^{39}Ar$ hornblende ages: implications for ocean-climate variability during last deglaciation. Earth Planet. Sci. Lett. 375, 441–449.
Kowalewski, M., Rimstidt, J.D., 2003. Average lifetime and age spectra of detrital grains: toward a unifying theory of sedimentary particles. J. Geol. 111, 427–439.
Kyle, P.R., 2013. A. McMurdo volcanic group western Ross embayment. In: LeMasurier, W. E., Thomson, J.W., Baker, P.E., Kyle, P.R., Rowley, P.D., Smellie, J.L., Verwoerd, W.J. (Eds.), Volcanoes of the Antarctic Plate and Southern Oceans. American Geophysical Union, Washington, D.C.
Ledent, D., Patterson, C., Tilton, G.R., 1964. Ages of zircon and feldspar concentrates from North American beach and river sands. J. Geol. 72, 112–122.
Liu, X., Jahn, B., Zhao, Y., Li, M., Li, H., Liu, X., 2006. Late Pan-African granitoids from the Grove Mountains, East Antarctica: age, origin and tectonic implications. Precambrian Res. 145, 131–154.
Liu, X., Zhao, Y., Zhao, G., Jian, P., Xu, G., 2007. Petrology and geochronology of granulites from the McKaskle Hills, Eastern Amery Ice Shelf, Antarctica, and implications for the evolution of the Prydz Belt. J. Petrol. 48, 1443–1470.
Ludwig, K.R., 2003. User's manual for Isoplot/Ex version 3.00. A geochronological toolkit for Microsoft Excel. Berkeley Geochronology Center Special Publication. 4, p. 72.
Marschall, H.R., Hawkesworth, C.J., Storey, C.D., Dhuime, B., Leat, P.T., Meyer, H.-P., Tamm-Buckle, S., 2010. The annandagstoppane granite, East Antarctica: evidence for Archaean intracrustal recycling in the Kaapvaal–Grunehogna craton from zircon O and Hf isotopes. J. Petrol. 51, 2277–2901.
McDougall, I., Harrison, T.M., 1999. Geochronology and Thermochronology by the 40Ar/39Ar Method. Oxford University Press, New York.
Meert, J.G., 2003. A synopsis of events related to the assembly of eastern Gondwana. Tectonophysics 362, 1–40.
Meert, J.G., Torsvik, T.H., 2003. The making and unmaking of a supercontinent: Rodinia revisited. Tectonophysics 375, 261–288.
Ménot, R.P., Duclaux, G., Peucat, J.J., Rolland, Y., Guillot, S., Fanning, M., Bascou, J., Gapais, D., Pêcher, A., 2007. Geology of the Terre Adélie Craton (135–146° E). Antarctica: A Keystone in a Changing World Online Proceedings of the 10th ISAES: U.S. Geological Survey Open-File Report 2007-1047 Extended Abstract 048 (3 pp.).
Mezger, K., Krogstad, E.J., 1997. Interpretation of discordant U–Pb zircon ages: an evaluation. J. Metamorph. Geol. 15, 127–140.
Mikhalsky, E.V., Beliatsky, B.V., Savva, E.V., Wetzel, H.U., Federov, L.V., Weiser, T., Hahne, K., 1997. Reconnaissance geochronologic data on polymetamorphic and igneous rocks of the Humboldt Mountains, central Queen Maud Land, East Antarctica. In: Ricci, C.A. (Ed.), The Antarctic Region: Geological Evolution and Processes. Terra Antartica Publication, Sienea, pp. 45–54.
Millar, I.L., Pankhurst, R.J., 1987. Rb–Sr geochronology of the region between the Antarctic Peninsula and the Transantarctic Mountains: Haag Nunataks and Mesozoic granitoids. In: McKenzie, G.D. (Ed.), Gondwana Six: Structure, Tectonics and Geophysics: Geophysical Monograph. 40. American Geophysical Union, pp. 151–160.
Minor, D.R., Muakas, S.B., 1997. Zircon U–Pb and hornblende $^{40}Ar–^{39}Ar$ ages for the Dufek layered mafic intrusion, Antarctica: implications for the age of the Ferrar large igneous province. Geochim. Cosmochim. Acta 61, 2497–2504.
Möller, A., Post, N.J., Hensen, B.J., 2002. Crustal residence history and garnet Sm–Nd ages of high-grade metamorphic rocks from the Windmill Islands area, East Antarctica. Int. J. Earth Sci. 91, 993–1004.
Morton, A.C., 1984. Stability of detrital heavy minerals in Tertiary sandstones from the North Sea Basin. Clay Miner. 19, 287–308.
Morton, A.C., 1991. Geochemical studies of detrital heavy minerals and their application to provenance studies. In: Morton, A.C., Todd, S.P., Haughton, P.D.W. (Eds.), Developments in Sedimentary Provenance Studies. Geological Society of London Special Publications, London, pp. 31–45.
Nesbitt, H.W., Young, G.M., 1996. Petrogenesis of sediments in the absence of chemical weathering: effects of abrasion and sorting on bulk composition and mineralogy. Sedimentology 43, 341–358.
Nesse, W.D., 2000. Introduction to Mineralogy. Oxford University Press, New York.
Oliver, R.L., Fanning, C.M., 1997. Australia and Antarctica. Precise correlation of Palaeoproterozoic terrains. In: Riccia, C.A. (Ed.), Antarctic Region: Geological Evolution and Processes. Terra Antartica Publishers, Siena, pp. 163–172.
Palmer, E.F., Licht, K.J., Swope, R.J., Hemming, S.R., 2012. Nunatak moraines as repository of what lies beneath the East Antarctic ice sheet. GSA Spec. Pap. 487, 97–104.
Paulsson, O., Austrheim, H., 2003. A geochronological and geochemical study of rocks from Gjelsvikfjella, Dronning Maud Land, Antarctica — implications for Mesoproterozoic correlations and assembly of Gondwana. Precambrian Res. 125, 113–138.
Peck, V.L., Hall, I.R., Zahn, R., Grousset, F., Hemming, S.R., Scourse, J.D., 2007. The relationship of Heinrich events and their European precursors over the past 60 ka BP: a muti-proxy ice-rafted debris provenance study in the North East Atlantic. Quat. Sci. Rev. 26, 862–875.
Peters, M., Haverkamp, B., Emmermann, R., Kohen, H., Weber, K., 1991. Palaeomagnetism, K–Ar dating and geodynamic setting of igneous rocks in western and central Neuschwabenland, Antarctica. In: Thomson, M.R.A., Crame, J.A., Thomson, J.W. (Eds.), Geological Evolution of Antarctica. Cambridge University Press, pp. 549–555.
Pettijohn, F.J., 1941. Persistance of heavy minerals and geologic age. J. Geol. 49, 610–625.
Peucat, J.J., Ménot, R.P., Monnier, O., Fanning, C.M., 1999. The Terre Adélie basement in the East-Antarctica shield: geological and isotopic evidence for a major 1.7 Ga thermal event; comparison with the Gawler Craton in South Australia. Precambrian Res. 94, 205–224.
Peucat, J.J., Capdevila, R., Fanning, C.M., Ménot, R.-P., Pécora, L., Testut, L., 2002. 1. 60 Ga felsic volcanic blocks in the moraines of the Terre Adélie craton, Antarctica: comparisons with the Gawler Range volcanics South Australia. Aust. J. Earth Sci. 49, 831–845.
Phillips, G., Wilson, C.J.L., Phillips, D., Szczepanski, S.K., 2007. Thermochronological ($^{40}Ar/^{39}Ar$) evidence of Early Paleozoic basin inversion within the southern Prince Charles Mountains, East Antarctica: implications for East Gondwana. J. Geol. Soc. Lond. 164, 771–784.
Pierce, E.L., Williams, T., van de Flierdt, T., Hemming, S.R., Steven, S.L., Brachfeld, S.A., 2011. Characterizing the sediment provenance of East Antarctica's weak underbelly: the Wilkes and Aurora sub-glacial basins. Paleoceanography 26, PA4217.
Poldervaart, A., 1955. Zircon in rocks, 1: sedimentary rocks. Am. J. Sci. 253, 433–463.
Poldervaart, A., 1956. Zircon in rocks. 2. Igneous rocks. Am. J. Sci. 254.
Post, N.J., 2000. Unravelling Gondwana Fragments; an Integrated Structural, Isotopic and Petrographic Investigation of the Windmill Islands, Antarctica. University of New South Wales.

Post, N.J., Hensen, B.J., Kinny, P.D., 1996. Two metamorphic episodes during a 1340–1180 Ma convergent tectonic event in the Windmill Islands, East Antarctica. In: Ricci, C.A. (Ed.), The Antarctic Region; Geological Evolution and Processes; Proceedings of the VII ISAES, pp. 157–161.
Reiners, P.W., Campbell, I.H., Nicolescu, S., Allen, C.M., Hourigan, J.K., Garver, J.I., Mattinson, J.M., Cowan, E.S., 2005a. (U–Th)/(He–Pb) double dating of detrital zircons. Am. J. Sci. 305, 259–311.
Reiners, P.W., Ehlers, T.A., Zeitler, P.K., 2005b. Past, present, and future of thermochronology. Rev. Mineral. Geochem. 58, 1–18.
Renne, P.R., Becker, T.A., Swapp, S.M., 1990. 40Ar/39Ar laser-probe dating of detrital micas from the Montgomery Creek formation, northern California: clues to provenance, tectonics and weathering processes. Geology 18, 563–566.
Renne, P.R., Swisher, C.C., Deino, A.L., Karner, D.B., Owens, T.L., DePaolo, D.J., 1998. Intercalibration of standards, absolute ages and uncertainties in $^{40}Ar/^{39}Ar$ dating. Chem. Geol. 145, 117–152.
Rilling, S.E., Mukasa, S.B., Wilson, T.J., Lawver, L.A., 2007. $^{40}Ar–^{39}Ar$ age constraints on volcanism and tectonism in the Terror Rift of the Ross Sea, Santa Barbara, CA. ,p. 4.
Rivers, T., 1997. Lithotectonic elements of the Grenvill Province: review and tectonic implications. Precambrian Res. 86, 117–154.
Roy, M., Clark, P.U., Duncan, A.R., Hemming, S.R., 2007a. Insights into the late Cenozoic configuration of the Laurentide ice sheet from $^{40}Ar/^{39}Ar$ dating of glacially transported minerals in midcontinent tills. Geochem. Geophys. Geosyst. 8.
Roy, M., van de Flierdt, T., Hemming, S.R., Goldstein, S.L., 2007b. $^{40}Ar/^{39}Ar$ ages of hornblende grains and bulk Sm/Nd isotopes of circum-antarctic glacio-marine sediments: implications for sediment provenance in the Southern Ocean. Chem. Geol. 244, 507–519.
Samson, S.D., Alexander, E.C., 1987. Calibration of the interlaboratory $^{40}Ar/^{39}Ar$ dating standard, MMhb-1. Chem. Geol. 66.
Sheraton, J.W., Black, L.P., Tindle, A.G., 1992. Petrogenesis of plutonic rocks in a Proterozoic granulite-facies terrane — the Bunger Hills, East Antarctica: chemical geology. Chem. Geol. 97, 163–198.
Sheraton, J.W., Tingey, R.J., Black, L.P., Oliver, R.L., 1993. Geology of the Bunger Hills area, Antarctica: implications for Gondwana correlations. Antarct. Sci. 5, 85–102.
Silver, L.T., Deutsch, S., 1963. Uranium–lead isotopic variations in zircons: a case study. J. Geol. 71.
Small, D., Parrish, R.R., Austin, W.E.N., Cawood, P.A., Rinterknecht, V., 2013. Provenance of North Atlantic ice-rafted debris during the last deglaciation — a new application of U–Pb rutile and zircon geochronology. Geology 41, 155–158.
Steiger, R.H., Jäger, E., 1977. Subcommission on geochronology: convention on the use of decay constants in geo- and cosmochronology. Earth Planet. Sci. Lett. 36, 359–362.
Storey, B.C., Pankhurst, R.J., Johnson, A.C., 2004. The Grenville Province within Antarctica: a test of the SWEAT hypothesis. J. Geol. Soc. 151, 1–4.
Stüwe, K., Oliver, R., 1989. Geological history of Adélie Land and King George V Land, Antarctica: evidence for a polycyclic metamorphic evolution. Precambrian Res. 43, 317–334.
Tatsumoto, M., Patterson, C., 1964. Age studies of zircon and feldspar concentrates from the Franconia Sandstone. J. Geol. 2, 232–242.
Tessensohn, F., Henjes-Kunst, F., 2005. Northern Victoria Land terranes, Antarctica: far travelled or local products? Geol. Soc. Lond. Spec. Publ. 246, 275–291.
Thomas, W.A., 2011. Detrial-zircon geochronology and sedimentary provenance. Lithosphere 3, 304–308.
Thomas, R.J., Cornell, D.H., Armstrong, R.A., 1999. Provenance age and metamorphic history of the Quha Formation, Natal Metamorphic Province: a U–Th–Pb zircon SHRIMP study. S. Afr. J. Geol. 102, 83–88.
Thomson, S.N., Reiners, P.W., Hemming, S.R., Gehrels, G., 2013. The contribution of glacial erosion to shaping the hidden landscape of East Antarctica. Nat. Geosci. 6, 203–207.
Thoulet, J., 1913. Notes de lithologies sous-marine. Annual Ins. Océanographie. 5.
Tingey, J.R., 1991. The regional geology of Archean and Proterozoic rocks in Antarctica. In: Tingey, J.R. (Ed.), The Geology of Antarctica. Clarendon Press, Oxford, pp. 1–73.
Tochilin, C.J., Reiners, P.W., Thomson, S.N., Gehrels, G., Hemming, S.R., Pierce, E.L., 2012. Erosional history of the Prydz Bay sector of East Antarctica from detrital apatite and zircon geo- and thermochronology multidating. Geochem. Geophys. Geosyst. 13, 21.
Tong, L., 2004. Metamorphism of Granulite Facies Metapelits. University of Melbourne.
Tong, L., Liu, X., Zhang, L., Chen, H., 1998. The $^{40}Ar–^{39}Ar$ ages of hornblendes in Grt–Pl-bearing amphibolite from the Larsemann Hils, East Antarctica and their geological implications. Chin. J. Polar Sci. 9, 79–91.
Tong, L., Wilson, C.J.L., Liu, X., 2002. A high-grade event of ~1100 Ma preserved within the ~500 Ma mobile belt of the Larsemann Hills, East Antarctica: further evidence from $^{40}Ar/^{39}Ar$ dating. Terra Antarct. 9, 73–86.
Tribuzio, R., Tiepolo, M., Fiameni, S., 2008. A mafic–ultramafic cumulate sequence derived from boninite-type melts (Niagara Icefalls, northern Victoria Land, Antarctica). Contrib. Mineral. Petrol. 155, 619–633.
van de Flierdt, T., Hemming, S.R., Goldstein, S.L., Gehrels, G.E., Cox, S.E., 2008. Evidence against a young volcanic origin of the Gamburtsev Subglacial Mountains, Antarctica. Geophys. Res. Lett. 35, 1–6.
Vaughan, A.P.M., Storey, B.C., 2000. The eastern Palmer Land shear zone: a new terrane accretion model for the Mesozoic development of the Antarctic Peninsula. Geol. Soc. London 157, 1243–1256.
Veevers, J.J., 2003. Pan-African is Pan-Gondwanaland: oblique convergence drives rotation during 650–500 Ma assembly. Geology 31, 501–504.
Veevers, J.J., 2004. Gondwanaland from 650–500 Ma assembly through 320 Ma merger in Pangea to 185–100 Ma breakup: supercontinental tectonics via stratigraphy and radiometric dating. Earth-Sci. Rev. 68, 1–132.
Veevers, J.J., 2012. Reconstructions before rifting and drifting reveal the geological connections between Antarctica and its conjugates in Gondwanaland. Earth Sci. Rev. 111, 249–318.
Veevers, J.J., Saeed, A., 2011. Age and composition of Antarctic bedrock reflected by detrital zircons, erratics, and recycled microfossils in the Prydz Bay–Wilkes Land–Ross Sea–Marie Byrd Land sector (70°–240°E). Gondwana Res. 20, 710–738.
Wang, Y., Liu, D., Chung, S.-L., Tong, L., Ren, L., 2007. Shrimp zircon age constraints from the Larsemann Hills region, Prydz Bay, for a late Mesoproterozoic to Early Neoproterozoic tectono-thermal event in East Antarctica. Am. J. Sci. 308.
Williams, T., van de Flierdt, T., Chung, E., Roy, M., Hemming, S.R., Goldstein, S.L., 2010. Evidence for iceberg armadas from East Antarctica in the Southern Ocean during the late Miocene and early Pliocene. Earth Planet. Sci. Lett. 290, 351–361.
Wilson, C.J.L., Quinn, C., Tong, L., Phillips, D., 2007. Early Palaeozoic intracratonic shears and post-tectonic cooling in the Rauer Group, Prydz Bay, East Antarctica constrained by $^{40}Ar/^{39}Ar$ thermochronology. Antarct. Sci. 19, 339–353.
Zeh, A., Millar, I.L., Kroner, U., Görz, I., 1999. The structural and metamorphic evolution of the Northern Haskard Highlands, Shackleton Range, Antarctica. Terra Antarct. 6, 249–268.
Zhao, Y., Song, B., Wang, Y., Ren, L., Li, J., Chen, T., 1992. Geochronology of the late granite in the Larsemann Hills, East Antarctica. In: Kaminuma, K., Shiraishi, K. (Eds.), Recent Progress in Antarctic Earth Science. Terra Scientific Publishing, Tokyo.
Zhao, Y., Liu, X.H., Wang, S.C., Song, B., 1997. Syn- and post-tectonic cooling and exhumation in the Larsemann Hills, East Antarctica. Episodes 20, 122–127.